

# Human Activity Recognition in an Open World

**Derek S. Prijatelj**

**Samuel Grieggs**

**Jin Huang**

*Department of Computer Science and Engineering*

*University of Notre Dame*

*Notre Dame, IN 46556, USA*

DPRIJATE@ND.EDU

SGRIEGGS@ND.EDU

JHUANG24@ND.EDU

**Dawei Du**

**Ameya Shringi**

**Christopher Funk**

*Kitware, Inc.*

*1712 Route 9, Suite 300, Clifton Park, NY 12065, USA*

DAWEI.DU@KITWARE.COM

AMEYA.SHRINGI@KITWARE.COM

CHRISTOPHER.FUNK@KITWARE.COM

**Adam Kaufman**

**Eric Robertson**

*PAR Government*

*421 Ridge St, Rome, NY 13440, USA*

ADAM\_KAUFMAN@PARTECH.COM

ERIC\_ROBERTSON@PARTECH.COM

**Walter J. Scheirer**

*Department of Computer Science and Engineering*

*University of Notre Dame*

*Notre Dame, IN 46556, USA*

WALTER.SCHEIRER@ND.EDU

## Abstract

Managing novelty in perception-based human activity recognition (HAR) is critical in realistic settings to improve task performance over time and ensure solution generalization outside of prior seen samples. Novelty manifests in HAR as unseen samples, activities, objects, environments, and sensor changes, among other ways. Novelty may be task-relevant, such as a new class or new features, or task-irrelevant resulting in nuisance novelty, such as never before seen noise, blur, or distorted video recordings. To perform HAR optimally, algorithmic solutions must be tolerant to nuisance novelty, and learn over time in the face of novelty. This paper 1) formalizes the definition of novelty in HAR building upon the prior definition of novelty in classification tasks, 2) proposes an incremental open world learning (OWL) protocol and applies it to the Kinetics datasets to generate a new benchmark KOWL-718, 3) analyzes the performance of current state-of-the-art HAR models when novelty is introduced over time, 4) provides a containerized and packaged pipeline for reproducing the OWL protocol and for modifying for any future updates to Kinetics. The experimental analysis includes an ablation study of how the different models perform under various conditions as annotated by Kinetics-AVA. The protocol as an algorithm for reproducing experiments using the KOWL-718 benchmark will be publicly released with code and containers at <https://github.com/prijatelj/human-activity-recognition-in-an-open-world>. The code may be used to analyze different annotations and subsets of the Kinetics datasets in an incremental open world fashion, as well as be extended as further updates to Kinetics are released.

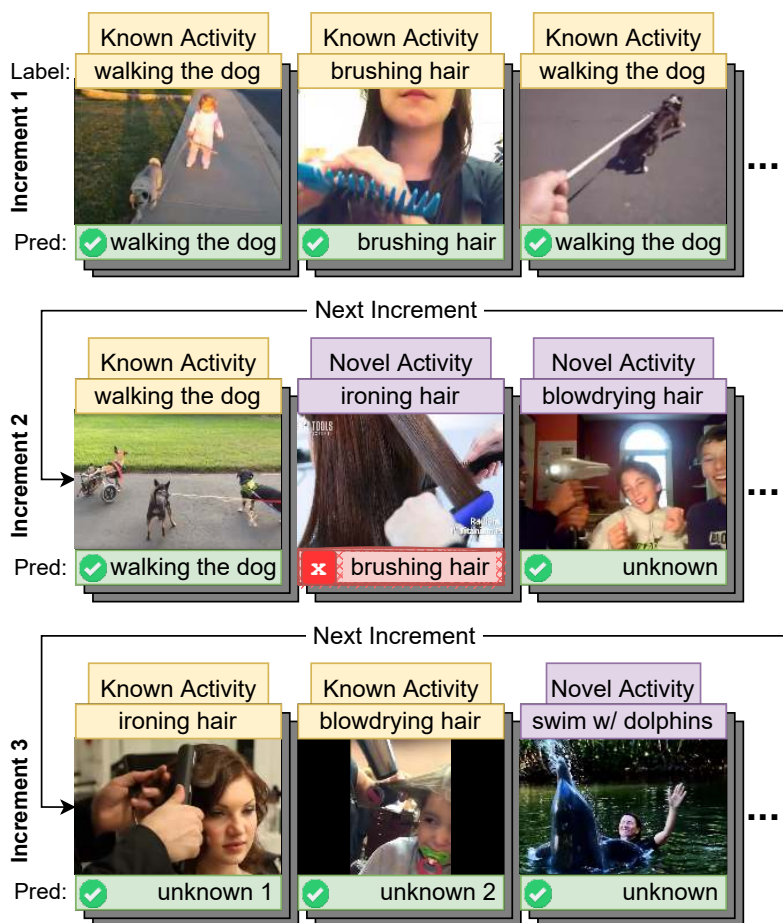


Figure 1: An example of open world visual human activity recognition starting from Kinetics-400 (Kay et al., 2017) known activities and **incrementally learning novel activities** from Kinetics-700-2020 (Carreira et al., 2019; Smaira et al., 2020). In Increment 2, without handling novelty, all unknown activities would be misclassified, when it is more correct to label them as “unknown.” In an open world, learning unknown activities is desired, as in Increment 3 where “ironing hair” and “blowdrying hair” have been learned by the predictor and represented with stand-in unknown classes 1 and 2 to differentiate from the general unknown class. These stand-in labels remain until the predictor is given (or determines) a human readable label.

## 1. Introduction

Human activities consist of a multitude of visual phenomena whose mappings to semantic classes are noisy and uncertain. These activities may vary from swimming alone in the ocean, to playing in team sports such as football, or to reading an academic article. Not only can the activities be different, but the environments in which they take place may be highly varied (Minh Dang, Min, Wang, Jalil Piran, Hee Lee, & Moon, 2020). The task of Human Activity Recognition (HAR) consists of recognizing and classifying these activities in visual recordings (Beddiar, Nini, Sabokrou, & Hadid, 2020). Given the extent of possible human activities and the variation within a single activity, datasets are often under-sampled representations of the task, which results in a problem of generalization for the predictors that perform HAR when they encounter novel human activities or

even novel instances of known human activities. This necessitates learning over time as more data is released and serves as a practical example of incremental open world learning.

The Open World Learning (OWL) setting (Bendale & Boulton, 2015; Boulton, Cruz, Dhamija, Gunther, Henrydoss, & Scheirer, 2019; Langley, 2020) is designed to expect novelty, including the lack of exhaustive samples for known classes and the lack of any samples for unseen, novel classes. As such, OWL presents a more practical experimental setting for HAR that has yet to be introduced in the HAR literature. OWL may take on the form of incremental learning (Belouadah, Popescu, & Kanellos, 2021) where new batches of samples are made available over the time-steps. The task is to perform HAR and learn the activity classes over time as new samples are introduced. An instantiation of HAR can be found in the Kinetics datasets, which have been released since 2017, introducing new classes and samples, including Kinetics-400 (Kay et al., 2017), Kinetics-600 (Carreira, Noland, Banki-Horvath, Hillier, & Zisserman, 2018), Kinetics-700-2020 (Carreira et al., 2019; Smaira et al., 2020), and Kinetics-AVA (Li, Thotakuri, Ross, Carreira, Vostrikov, & Zisserman, 2020). For brevity, if we refer to Kinetics-700, we mean the 2020 updated version. Ideally, HAR predictors should be comparable and generalize across the Kinetics datasets. Given the inherent lack of samples to characterize all human activities, HAR predictors must account for learning over time as data is made available, as in the case of the Kinetics and other datasets, and these predictors should adapt to novelties that affect task performance (Bendale & Boulton, 2015). To evaluate such predictors, we define an OWL protocol with accompanying code to configure and run a Kinetics Open World Learning (KOWL) experiment.

**Contributions:** To better evaluate the generalization of predictors in Open World HAR when encountering novelty, this paper introduces:

1. A formal definition of Open World HAR in Section 3 as an instantiation of the newly introduced framework by (Boulton, Grabowicz, Prijatelj, Stern, Holder, Alspector, Jafarzadeh, Ahmad, Dhamija, Li, Cruz, Shrivastava, Vondrick, & Walter, 2021), which establishes a common language for novelty across AI domains;
2. An OWL protocol in Section 4 as an extension to (Dhamija, Ahmad, Schwan, Jafarzadeh, Li, & Boulton, 2021) to create experiments to analyze novelty in HAR datasets, applied to Kinetics 400 (Kay et al., 2017), 600 (Carreira et al., 2018), and 700-2020 (Smaira et al., 2020) to create KOWL-718, accompanied by baseline predictors for benchmarking;
3. An detailed analysis in Section 5 of the performance of pre-existing state-of-the-art visual HAR models in the presence of novelty, including X3D (Feichtenhofer, 2020) and TimeFormer (Bertasius, Wang, & Torresani, 2021).
4. Pipeline code for configuring and running the open world HAR experiments<sup>1</sup> with a Docker image to both reproduce the Kinetics experiments below, as well as enable any configuration for open world Kinetics experiments in the future.

## 2. Background and Related Work

Fundamentally, novelty is anything that is new to something else. This could be related to the task being learned, such as a sample of a new class in the evaluation set, or new features that

---

1. Code repository with containers for reproducing and extending: <https://github.com/prijatelj/human-activity-recognition-in-an-open-world>

correlate strongly with a known class (Chalmers, 2006). Such things are deemed “task-relevant” if they contain information to accomplish the task (Tishby, Pereira, & Bialek, 1999; Gershman & Niv, 2015). Novelty can also be task-irrelevant, for example the color of one’s new clothes is a feature of a video that should be mostly uncorrelated with the activity of standing in place. Such task-irrelevant novelty is termed “nuisance novelty” and its affect on task performance is to be minimized. Such concepts of novelty have been defined in a formal abstraction with a relation to agents performing their tasks in general AI settings by (Boult et al., 2021). Note that (Boult et al., 2021) define their abstraction referring to the task’s algorithmic solution as an “agent,” where in this work we refer to them as “predictors.” The primary actions of the predictors observed in this work are their predicted classification probability vectors and an optional feedback request through the ordering of the sample identifiers based on priority of interest to the predictor.

Open Set Recognition (Scheirer, Rocha, Sapkota, & Boult, 2013; Geng, Huang, & Chen, 2021), Anomaly Detection (Pang, Shen, Cao, & Hengel, 2021; Ruff, Kauffmann, Vandermeulen, Montavon, Samek, Kloft, Dietterich, & Müller, 2021), Novelty Detection (Roitberg, Al-Halah, & Stiefelhagen, 2018), and Out-of-Distribution Detection (Zaemzadeh, Bisagno, Sambugaro, Conci, Rahnavard, & Shah, 2021) are all intended to detect when a sample occurs that contains novel information that was not represented by the prior data. For simplicity, this paper refers to these similar tasks solely as “novelty detection.” In terms of classification tasks, as in Open Set Recognition, a sample with a large amount of novel information cannot be reliably classified as a known class, and instead should be labeled as an unknown class. Novelty detection does not involve incremental learning to adapt to novelty; it only involves the detection of novelty. This may be seen as detecting out-of-distribution samples based on a single time-step.

OWL (Boult et al., 2019; Langley, 2020; Geng et al., 2021) is an example of learning-based classification or recognition with novelty in mind. OWL is the natural extension of novelty detection where new classes are learned alongside the known classes. Recent work has proposed a practical OWL protocol for image classification (Dhamija et al., 2021) as an extension of Incremental Classifier and Representation Learning (Rebuffi, Kolesnikov, Sperl, & Lampert, 2017), but no OWL protocol, benchmark dataset, or model exist for HAR. In this paper we extend OWL to HAR, a more visually complicated problem than static image classification. Our work contains multiple key differences from this prior work. The protocol we introduce below measures performance using a confusion matrix per time-step, which captures all the information for a single time-step between the predictor’s nominal output as the maximally likely activity class. Dhamija *et al.* only observe accuracy. In Section 5 we demonstrate why observing only accuracy as the single point-estimate measure of performance at a time-step is insufficient. Furthermore, Dhamija *et al.* only observe classification performance for known classes alone, known classes with a catch-all unknown class for others, and binary classification of novelty detection. Our protocol encourages looking at not only novelty detection, but also novelty recognition, which is the assessment of the predicted unknown class-clusters to define new classes that can be considered known information going forward. Incremental OWL is inherently a semi-supervised task and it is important to evaluate the quality of recognized unknown classes. Kinetics has been typically assessed using top-5 accuracy. Given this, our approach considers the top- $k$  ordered confusion matrices in which one may obtain the top- $k$  accuracy, along with the top-1 confusion matrix and its measures derived from it, as we do throughout this paper.

While the confusion matrix covers task performance at a single time-step (non-cumulative) or over multiple increments (cumulative), Dhamija *et al.* do not evaluate the reaction time of the

predictor to novelty occurring. We include details of a way to do so in Section 4.1. In addition, we also include the action predictors may take, the feedback request as explained in Section 4.2. Requested feedback may be limited in practice due to the cost of humans, especially human experts, annotating the samples. Due to this, we included an any % feedback experiment parameter where the evaluator limits the amount of labels the predictor may receive for their training set of the new increment. Given this limitation, the predictor is forced to order the samples it received within the current increment’s training set. This becomes a subtask to request the labels that enable more efficient learning of the task.

Another important distinction between the work of Dhamija *et al.* and our work is that we encourage the predictors to have no prior knowledge when being evaluated on this baseline, or at least to have an explicit disclaimer of their prior knowledge such that those predictors may be properly compared to similarly prior informed predictors. For this benchmark to assess the learning of this task as represented by this data, no prior knowledge should be used. Otherwise, the assessment is more about whether the prior knowledge shared information with this task or better enabled the learning of this task. This distinction is important, especially considering the current dominant trend in AI of using large pre-trained models for transfer learning to down-stream tasks (Qiu, Sun, Xu, Shao, Dai, & Huang, 2020).

There are some HAR works related to Open Set Recognition (Roitberg, Ma, Haurilet, & Stiefel-hagen, 2020; Gutoski, Lazzaretti, & Lopes, 2021; Brighi, Franco, & Maio, 2021; Inácio, Gutoski, Lazzaretti, & Lopes, 2021), but none that attempt to provide a benchmark or solution for OWL in HAR, which involves incremental learning in a world with unknown human activity classes and their associated videos. Three methods approach this goal. Deep Metric Learning for Open Set HAR (Gutoski et al., 2021) uses metric learning to improve feature representation models for open set recognition, but the associated experiments do not involve incremental learning. Activity Explorer (Brighi et al., 2021) is described as having an ability to recognize potentially new classes, but is only assessed within an OSR context, rather than in an OWL context. It does not include logic on how to update classes over time, leaving it to the human user. OSVidCap (Inácio et al., 2021) is for the task of Video Captioning, which is related to HAR, but is not HAR specifically. Like the other two approaches, it is evaluated in an Open Set Recognition mode, not OWL.

A feature representation space that generalizes to the task and captures the world’s task-relevant information is an important part in solving HAR with novelty. The state of representation learning consists of large semi-supervised deep neural networks with copious amounts of data (Radford, Kim, Hallacy, Ramesh, Goh, Agarwal, Sastry, Askell, Mishkin, Clark, Krueger, & Sutskever, 2021; Schiappa, Rawat, & Shah, 2022), or generative models that leverage adversarial examples or augmentations for contrastive learning (Ho & Vasconcelos, 2020). Feature representation is important for OWL because it determines what information is available to learn the task for the down-stream components, such as the classifier (see Figure 6). Not only do OWL classifiers need to be able to learn new classes over time, but ideally their representation learners must also be able to adapt to include missing task-relevant information. This is similar to the popular pretrained models in natural language processing where a semi-supervised model, such as a transformer, is pretrained on an upstream task with a large dataset and in doing so learns information relevant to many down-stream tasks (Qiu et al., 2020). With a feature representation that contains information not only relevant to the current downstream task but also contains possibly future relevant task information, the classifiers are able to distinguish between known and unknown, learning novel classes over time. Incremental learning model types that perform fine-tuning are one way to adapt the feature represen-

tation space over the increments (Belouadah et al., 2021). Frozen or fixed representations rely on a feature representation that already contains the information relevant to learning novel classes in the future, where any downstream fine-tuning or classifier changes will change their learned function to use task-relevant information in the feature representation ignored prior to the novel class being introduced, given the data processing inequality (Cover & Thomas, 1991).

### 3. Formalization of Open World HAR

(Boult et al., 2021) provided a convenient framework for formalizing novelty problems in AI. A formal definition of novelty for HAR provides a standardized way to communicate and understand the impact of novelty on the performance of a learning-based system meant to recognize activities. This enables informed discussion about the nuances of OWL, including new classes and new types of task-relevant phenomena such as new visual features, *e.g.*, associating the visual depiction of a football with the sport.

The formalization starts with defining a task. HAR follows the classification task definition of learning a mapping  $f \in \{F : \mathcal{X} \rightarrow \mathcal{Y}\}$  that is some deterministic function of the possible mappings of the space of possible visuals of human activity  $\mathcal{X}$  to the space of possible human activity classes  $\mathcal{Y}$ . This mapping is estimated by a predictor from paired data samples  $(x, y)$ : a video sample  $x \in \mathcal{X}$  and the most likely human activity class label  $y \in \mathcal{Y}$ .

As noted earlier, it is well understood that the sampling of videos is often incomplete, but hopefully is representative of a subset of the possible videos. Given the space of class labels  $y \in \mathcal{Y}$  is never complete in OWL, novel activity classes thus are possible in future encountered HAR video samples. As such, the learning of an optimal mapping of  $f$  from data persists over time in OWL where one of the class labels stands for the unknown classes. This unknown class is used to represent the detection of novel classes. A HAR predictor’s output space or prediction space  $\hat{\mathcal{Y}}$  overlaps with the class space  $\mathcal{Y}$ .

In addition to this task, let there be novelty spaces in which the phenomena of the task occur. A novelty space includes:

- **State Space:** A measurable space in which the states  $s \in \mathcal{S}$  associated with various activities occur.
- **Dissimilarity Measure:** The quantification of how different states are to one another, possibly with a threshold for binary dissimilarity decisions and possibly task-specific to ignore some task-irrelevant phenomena.
- **Regret Measure:** The quantification of how undesirable a predictor’s  $\hat{Y}$  decision or the resulting state of that decision is relative to the task.
- **Experience:** A time-indexed history of the states that have occurred over time.
- **State Transition Function:** a function that moves from the current state to the next state given a change in time or an action taken by the predictor. In HAR, the time-step  $t$  corresponds to the index of the current sample and the predictor decides the class, detects novelty, possibly updates its state, and, if possible, may request feedback.

Novelty within this space is then determined by a new state that is significantly dissimilar based on the the Dissimilarity Measure to the states recorded in the prior Experience. Following (Boult et al.,

2021), HAR may be defined with three novelty spaces: 1) World space, 2) Observation space, and 3) Predictor space. Examples of the different subsets of novelty associated with these spaces are provided in Appendix B.

Our paper primarily focuses on the spaces in which novelty may occur related to classifying human activities, all of which were mentioned earlier: the input space  $\mathcal{X}$ , the predictor output space  $\hat{\mathcal{Y}}$ , and the ground truth target label space  $\mathcal{Y}$  obtained from a dataset. The relation of these to the primary three is as follows:

- The world defines that which is considered the truth to be learned, as defined by the dataset, meaning the paired mapping of video  $x$  to ground truth label  $y$ . The dataset as in order of presentation to the predictor forms the world experience. The order of presentation is based on the chosen experimental design and serves as the state transition function of the observed world. The regret measures are based on the relative comparison of predictions to the ground truth labels. Section 4.1 goes into explicit detail for any KOWL experiment. In this paper, all of these parts are controlled and executed by the “evaluator,” as seen in Figure 2, which is the algorithmic execution of the experiment.
- The observation space relates to how these human activities were captured visually, such as camera sensors. The original dataset determines the source of the visual recordings and may include any metadata defining those recordings. This is where nuisance novelty occurs, including never before experienced perspective rotations, hue shifts, blurs and noise.
- The predictor space consists of the predictor’s output space, experience, and internal state. Internal regret measures are those such as the optimization function in which the predictor optimizes as it learns, such as losses for neural networks. State transition functions for the predictor are its update functions as it receives videos and any feedback from the evaluator. See Section 4.4 for the complete abstraction and Section 5.1 for examples.

More detailed explanations of the world, observation, and predictor spaces as structured in (Boult et al., 2021) for defining novelty in HAR are available in the Appendices A and B.

### 3.1 Nuisance Novelty

It is important in all learning tasks to maximize the task-relevant information in the predictions and filter out the task-irrelevant information (Tishby et al., 1999), as measured by correlation measures of the predictions to the ground truth labels. Task-irrelevant information is noise or other irrelevant phenomena that occurs in the world and is possibly captured by the sensor. Nuisance novelties are novel task-irrelevant phenomena that have never before been encountered and which the predictor is to be tolerant to and maintain task performance. An example in HAR is that if someone is dancing, then in general their clothes should not be a strongly correlated feature to the recognized activity of dancing for the predictor to generalize across dancing videos. Nuisance novelty is defined in (Boult et al., 2021) as a novelty for which a pair of regret measures significantly disagree. In this example, the predictor may falsely detect novelty with respect to a new activity class when in reality it is only someone dancing in a never-before-seen colored shirt and the activity class label is still dancing.

Often is the case that some novelty may occur in the world, such as a sensor being knocked over and the visual input being rotated. The input being rotated is novel if rotations were never seen in training, but if all of the actions being recorded are known, then the predictor is desired

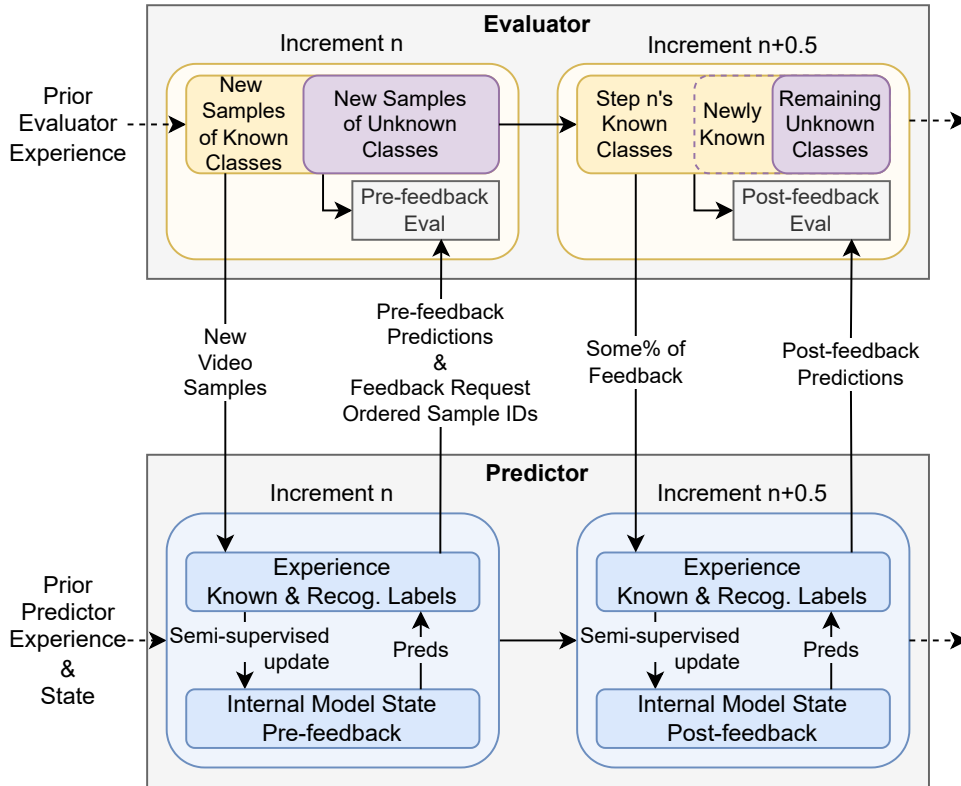


Figure 2: A single  $n$ -th increment of the OWL protocol depicting the exchange of data, state, and updating internal state for both the evaluator and the predictor. An increment consists of a pre-feedback phase (whole step  $n$ ) and a post-feedback phase (half step  $n + 0.5$ ), if any feedback given. On the  $n$ -th increment, new sample data is given from the evaluator to the predictor without any labels. The predictor performs any internal updates given this new unlabeled data, such as un- or semi-supervised learning, and returns its predictions. The predictor also returns the order of the samples it would like to receive feedback for. The evaluator evaluates the pre-feedback predictions and if it gives any feedback will note the samples whose feedback were given in its experience. In the case of giving ground truth class labels, those labels are now deemed as known. The predictor may update its state given any feedback it receives and perform a post-feedback prediction, which is then evaluated again. The process repeats until the experiment’s increments are exhausted. At the initial increment, prior knowledge obtained from external data, such as feature representations from other models, needs to be explicitly stated and evaluated appropriately. See Section 4.4.

to be tolerant to rotations of its field of view. However, if this rotation causes the predictor to continuously detect novel classes, despite them being known, then this is a nuisance novelty as the desired world regret pertaining to the HAR task is low while the predictor’s regret is high as it deems task-irrelevant information as task-relevant. Predictors need to maintain task performance in the face of such nuisance novelties. Further explanations of the different types of novelty with human activity are provided in appendix B.

#### 4. Open World Learning Protocol for HAR

Any labeled HAR dataset may be partitioned in such a way that yields an OWL HAR dataset with increments that consist of videos with shared known activities and novel activities. The following



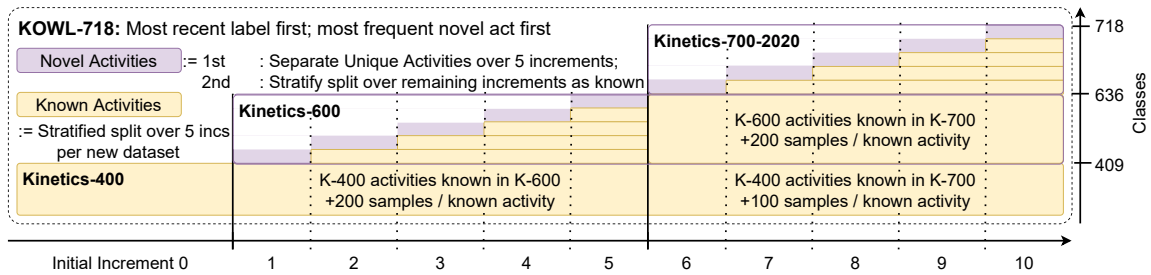


Figure 3: A visual representation of KOWL-718’s class density per increment as used in the experiments when the OWL protocol is applied to Kinetics-400 to Kinetics-700. The incremental learning uses a unified mapping of the Kinetics activity classes based on the most recent label first. Each increment contains a new set of unknown activities and the prior known activities persist as long as the original Kinetics datasets contained samples for them. The most frequent novel classes were introduced first within their respective dataset to help balance the samples over increments. See Section 4.

focuses on forming increments on the training data split. The validation and testing data splits may be split in the same way using the same class sets per increment such that they are aligned to the training data. Given the number of desired increments  $N$ , a labeled dataset that is an unordered sequence of pairs  $(x, y)$ , and the starting known label set  $K \subset \mathcal{Y}$ , the starting unknown label set  $U$  within the data is then the unique labels not contained within  $K$ , where  $U = \{y : y \notin K\}$ . The pairs with known labels may be split into the  $n$  increments in any way desired, such as stratified splits that maintain the balance of the known labels across the increments as much as possible with finite, discrete samples. With the known labels partitioned, the increments must also introduce novel classes when encountered. To do so, the unknown labels are separated uniformly across the  $N$  increments such that there are  $\lfloor \frac{|U|}{N} \rfloor$  unknown classes within in the first  $N - 1$  increments and the remaining unknown classes go into the final increment. At this point, every increment shares the known classes and has a subset of unknown classes disjoint to all other increments.

Given that we want the novel classes introduced at each increment to remain present in future increments, each increment’s unknown class samples need to be spread across the remaining increments that follow in time. To counteract class imbalance, it is useful to order the unknown classes by descending order of sample frequency and insert them as the most frequent unknown class first over the time ordered increments. The increment at time-step  $t$  has its unknown label set  $U_t$  that is stratified split into  $n - t$  splits. One of those splits remains in the current  $t$  increment. The other  $n - t - 1$  of those splits are added to the remaining future increments, where  $t \in \{0, 1, \dots, n - 2, n - 1\}$ . This results in an OWL HAR dataset that can be used to train and evaluate a predictor incrementally where sample index corresponds to time and there are  $N$  class distributional changes where novel classes are introduced, where the distribution in mind is the ground truth labels as a random variable whose set of possible labels at each increment grows. If training, validation, and testing splits are not predefined, each resulting increment from above may be split using any of the typical methodologies, such as 8:2 train-to-test ratios, or even multi-fold cross validation. If they are pre-defined, then validation and testing splits are separated into increments based on their classes corresponding to the classes in the training split, ensuring the validation and testing splits contain the training classes at each increment.

This protocol was used to construct a Kinetics Open World Learning experiment with 718 classes (KOWL-718) that followed the chronological release of the original datasets. By follow-

Increment	0	1	2	3	4	5	6	7	8	9	10
Classes											
Known	409	409	455	501	547	593	636	653	670	687	704
Novel	0	46	46	46	46	43	17	17	17	17	14
Train Samples											
Known	218371	16082	19148	24661	32391	44687	34287	36112	38527	41855	47128
Novel	0	3163	5513	7730	12298	25538	1870	2415	3331	5273	10144
Test* Samples											
Known	35256	1128	307	491	732	1096	4892	4990	5197	5473	5883
Novel	0	179	232	266	372	612	163	208	277	411	684

Table 1: **KOWL-718**’s resulting number of known and novel classes and their samples **per increment** using the configuration in Section 5: Most recent label first, first come first assigned data split, and most frequent novel class first per future dataset. The initial increment 0 uses the same splits as Kinetics-400 with 18,016 validation samples not listed above. The test split consists of Kinetics-600’s validation and test splits for the increments in range [1, 5] and the Kinetics-700-2020 validation split for increments in range [6, 10] given the Kinetics-700-2020 test set labels are not yet publicly released. Totalling 630,524 training samples and 68,849 test samples overall. \*See Appendix C.1 for further breakdown and a note on link rot where videos are lost.

ing the chronological release of the original datasets, the practical gathering of data and changing of a dataset over time is tracked. KOWL-718 starts with Kinetics-400 (Kay et al., 2017) as the initial increment, followed in order by Kinetics-600 (Carreira et al., 2018) split into 5 increments, and then Kinetics-700-2020 (Carreira et al., 2019; Smaira et al., 2020) split into 5 increments, as seen in Figure 3. The human activity labels between the original Kinetics datasets differ as more were added and existing classes were either removed, renamed, or reorganized. Some classes were separated into two or more classes, or samples that were in one class were moved to another. Given this inconsistency between labels, we constructed a Kinetics unified label set that prioritizes the most recent changes made to the datasets first: following Kinetics-700, then Kinetics-600, then Kinetics-400. This means that the samples that were in prior versions and are still in Kinetics-700 have a Kinetics-700 class, while the samples removed from future versions keep their most recent class. The resulting most-recent-first label set totals 718 activities. If following this order with consistent labeling, this ordered release of samples allows for predictors pretrained on the different original datasets to be used as checkpoints to start from for future predictors to skip prior increments, if so desired. The unified Kinetics criteria are as follows:

- **Label assignment:** *Most recent label first.* Thus, using Kinetics-700-2020 labels for all samples when available. If the samples in Kinetics-600 are not used in Kinetics-700-2020, then their activities as assigned from Kinetics-600 are used. Same applies for samples in Kinetics-400 that are not used in either Kinetics-600 or -700-2020. Under this configuration, such activities are not represented in later datasets, which matches the actual release of the data.
- **Data split assignment:** *First come, first assigned.* This follows how the data were released throughout the years, keeping persistent samples within their first assigned data split, and avoiding the issue of training samples from earlier Kinetics datasets being used in validation or test sets of later Kinetics datasets.

- **Introduction of novel activities:** *Most frequent first.* When adding a dataset as released in time, this means novel activities within Kinetics-600 and Kinetics-700-2020, the most frequent novel activity is introduced first such that there are more samples of that class across the  $N = 5$  increments. This aids in balancing out the number of samples across the remaining increments of a dataset.

While using the most recent labels means those re-labeled samples from older datasets are more accurate, it does result in class imbalance in the prior Kinetics datasets. As such, when using the OWL protocol to partition Kinetics-600 and -700 samples whose labels were fewer than the remaining increments, they were simply included only within the increment they were introduced in. This occurs specifically within the validation splits of these increments due to their smaller size relative to the training and testing splits. Given this we combined the validation and test splits of Kinetics-600 into our test set at those increments as seen in Figure 3 and Table 1. Due to using the most recent label first scheme, the Kinetics-400 and -600 training splits have classes that are not contained within their validation or testing sets throughout the incremental learning until the final increment. The resulting experimental dataset includes a starting increment consisting entirely of Kinetics-400 with a total of 10 following increments each with training and test splits determined by the original Kinetics-600 and -700 validation and test data using the most recent label first for each video. The Kinetics-700 validation data serves as the test data in KOWL-718 given the original test labels are not publicly released. Class balance is further detailed and visualized as a bar chart of occurrences in the Supplemental Material. An ablation study using annotations from Kinetics-AVA (Li et al., 2020) of the predictors based on certain video conditions such as the number of people within a key frame of a video is included in Section 5.3.

#### 4.1 Evaluation

Using an incremental OWL HAR dataset, incremental learning starts with fitting on the training data in the initial increment that includes the known classes in  $K$ , which matches typical supervised learning classification. As seen in Figure 2, the next increment’s data is introduced and the predictor is evaluated on all of that data prior to any feedback being provided, such as the ground truth labels. Novelty detection and recognition of human activities may now be evaluated. Recall that novelty detection is detecting when a sample belongs to an activity class unknown to the predictor at that time, and recall that novelty recognition is the classification of those detected unknown samples into potential class-clusters based on their feature representation and relation to known classes within the feature representation space. The prediction output may be a single nominal class or the probability vector of estimated likelihoods of the mutually exclusive classes. With the pre-feedback class predictions, the evaluator may measure the performance of the predictor on HAR classification, novelty detection, and novelty recognition. The confusion matrix captures all the information from a sampling of the marginal and joint distributions between the predicted most likely classes and the actual labels, which enables deriving measures often useful in evaluating classification and clustering. These include accuracy, Matthews Correlation Coefficient (MCC), and Normalized Mutual Information (NMI). Accuracy is easily human interpretable and assesses the correctness of the symbolic mapping of class labels, while MCC assess the linear correlations between the predictions and the ground truth labels, and NMI assesses both the linear and non-linear correlations (Kinney & Atwal, 2014). The types (**bold**) of evaluation measures necessary to make an informed assessment of the predictors are as follows along with our chosen measure (*italics*):

1. **Exact Symbol Matching: Accuracy:** The primary task, especially in classification, tends to desire the predictor to output agreed upon labels that are deemed useful to understand what the class pertains to. For example, we want unobfuscated labels of the activity being performed, such as “walking the dog” instead of “class\_379”. Accuracy is a common measure that evaluates how many samples have this correct label.
2. **Linear Correlation: Matthews Correlation Coefficient (MCC):** While easily human interpretable, at times the accuracy may measure larger values for ill-performing predictors, such as when a predictor outputs the most frequent label in an imbalanced label set. Linear correlation measures such as Pearson’s  $r$  coefficient or the equivalent Matthews Correlation Coefficient (MCC) will express low values for such undesired behavior. These values range from  $[-1, 1]$ , where -1 is inversely or negatively correlated, 0 is no correlation, and 1 is positively correlated.
3. **Task-Relevant Information: Arithmetic Mean of Entropies Normalized Mutual Information:** To further separate from the dependency on what is the exact symbol, non-linear correlations may be measured as well. Such measures place the importance on the information learned, which includes both linear and non-linear relationships, such as the mutual information between the predictions and the actual labels. While mutual information is the measure to use to determine how much of the task-relevant information was learned (Tishby et al., 1999), practically, the mutual information is unbounded and requires enough samples to properly estimate the actual information of the task and predictions. With this said, normalized variants of mutual information are available, such as the information quality ratio or the normalization by the arithmetic mean of the entropies, where the former is a more exact normalization when enough samples are available, and the latter is a better estimate when not enough samples are available, albeit not as interpretable in its reported ratio of information learned. When the mutual information is normalized, it may be reported within the ranges  $[0, 1]$ , where 1 indicates all task-relevant information was learned.

To observe only one of these measures ignores important performance information in the others. A well-performing predictor will maximize all of these point-estimate measures in- and out-of-sample.

Open world recognition, which is inherently a classification task, may be evaluated at each time step using a confusion matrix and any of its derived measures, such as those mentioned above. Depending on how classes are treated, one may observe the “raw” confusion matrix where the predicted labels and unknown ground truth labels remain as they were received. In this work we execute three different reductions of the confusion matrix’s labels to assess three specific subtasks listed below for open world recognition. These reductions are depicted in Figure 4. In addition to evaluating these three subtasks, a fourth subtask is necessary to assess the time-series information of reacting to novelty as it occurs through the incremental learning. In detail, the four subtasks are:

1. **Classification Task:** The primary activity classes of interest along with a single unknown class to account for any novel or unknown classes. To evaluate this, reduce the predictor’s recognized unknown classes into the general “unknown” class, indicating when the sample is deemed something other than that which is known and deemed important to the task. This is the typical assessment used in the original Kinetics protocol, minus the catch-all “unknown” class.

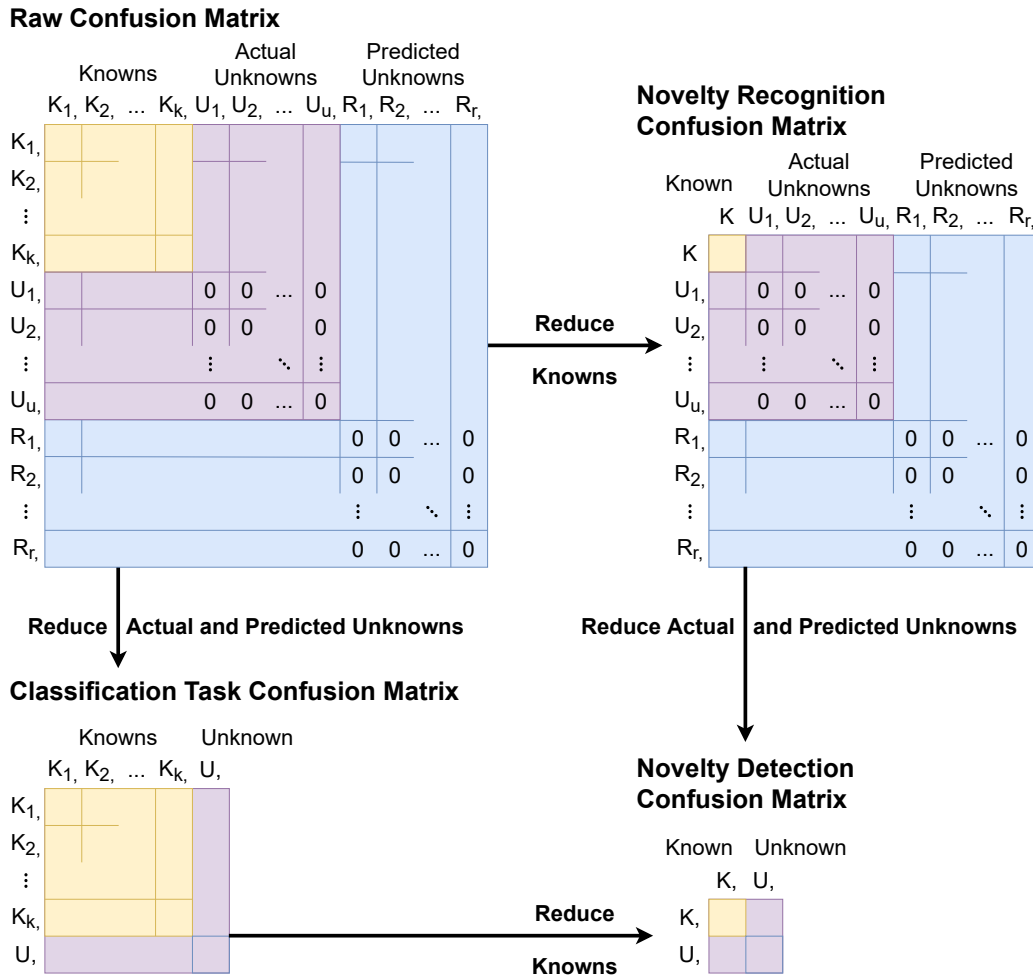


Figure 4: The raw confusion matrix and its reductions to assess performance of a predictor’s chosen activity classes at a time-step. The raw confusion matrix compares the actual known and unknown classes at a time-step to the predictor’s chosen activity class labels, including any recognized unknown classes. Given a predictor will never know the symbolic mapping of the actual unknowns at the current time-step, the confusion matrix will have sub-matrices of zero occurrences as indicated above. The reduction of known or unknown classes is performed to focus on the performance on subsets of classes or supersets in the case of detection. The confusion matrix captures all the information from a sampling of the marginal and joint distributions between the predictions and the actual labels, which enables deriving measures often useful to evaluate classification. See Section 4.1.

2. **Novelty Detection:** the binary classification of known vs. unknown. All known classes are reduced into a single “known” class, and all unknown classes are reduced into a single “unknown” class.
3. **Novelty Recognition:** the unsupervised class-clustering separate from the classification of the known classes. To focus on evaluating this, reduce all known classes into a single “known” class. The measures derived from the resulting confusion matrix must account for the class

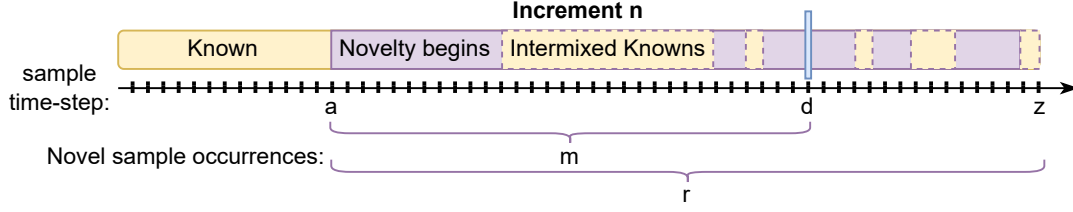


Figure 5: A visual depiction of the variables involved in the novelty reaction time measurement used in this work. An increment consists of samples that belong to intermixed known and novel classes.  $a$  is the sample index of the first instance of novelty in the increment.  $z$  is the index of a final instance of novelty in the increment.  $d$  is the index of the sample that the predictor detects as the first occurrence of novelty.  $m$  is the number of novel samples within the inclusive range  $[a, d]$ .  $r$  is the total number of novel samples within the increment. These are used in the harmonic mean in Equation 1.

labels not using the same symbols, even though they are the same cluster. This includes measures such as mutual information, as used in this work.

4. **Novelty Reaction Time:** The time it takes to react to novelty, which in the case of HAR is the reaction time, measured in samples, to detect novel activities after a single sample has occurred. Here, as in novelty detection, the known classes are reduced and the unknown classes are reduced, resulting in a binary classification assessment. The difference here is that the novelty reaction time measures how many samples pass after the occurrence of a novel activity’s sample.

We use the following procedure to measure novelty reaction time within a single increment whose variables are visualized in Figure 5: When the first novel sample occurs at the sample index  $a$ , record the number of novel samples  $m$  observed before the first sample index of novelty  $d$  is detected by the predictor at or after  $a$ . Let  $z$  be the final sample index of the increment and  $r$  be the total count of novel samples within the increment. The following harmonic mean is used to measure the novelty reaction time:

$$\left( \frac{\left( \frac{d-a}{z+1-a} \right)^{-1} + \left( \frac{m}{r} \right)^{-1}}{2} \right)^{-1} = \frac{2}{\frac{z+1-a}{d-a} + \frac{r}{m}} \quad (1)$$

where  $\frac{d-a}{z+1-a}$  is the fraction of samples that pass before novelty is first detected and  $\frac{m}{r}$  is the fraction of total novel samples that occur before detection occurs.  $z + 1$  is used because it reflects the total number of samples with a zero index. If novelty is never detected, then that corresponding fraction would be 1, otherwise it approaches 1 in the limit of  $z$  to infinity. Note that in the demonstration of KOWL-718 below, all samples in the increment are given to the predictor at once by the evaluator, rather than in “sub-increments” or batches.

All of these measurements require a clear distinction between what is known and what is novel. In the majority of this paper’s experimental demonstration in Section 5, the known classes are based on what activity class labels the predictor knows within its experience at that moment in time. All of their samples are thus deemed known or novel to the predictor based on this alone. This may be referred to as *novel-to-predictor*, or as predictor novelty. This is different from the novelty determined by if a predictor ever has experienced a sample from a certain novel class, which only

the evaluator could ever know without feedback to the predictor. This may be referred to as *novel-to-evaluator*, or as “actual novelty” as defined by (Boult et al., 2021). The evaluator may record the measurements from the above four subtasks above in either way as long as the reduction of knowns and unknowns follows the appropriate method of determining novelty for that case.

## 4.2 Requesting Feedback

After evaluating the predictor on the new increment’s data, feedback may be offered to it. The supervised incremental learning paradigm (Masana, Liu, Twardowski, Menta, Bagdanov, & van de Weijer, 2021; Losing, Hammer, & Wersing, 2018) releases all of the labels (100%) to the predictor for it to be fit. The experiment may also only release a subset of the labels, such as none (0% feedback) or partial feedback, such as 50% of the samples for this new increment. Our OWL protocol gives the predictor another subtask of requesting feedback for itself from the evaluator after every pre-feedback evaluation. This feedback request takes the form of an ordered list of the samples’ unique identifiers. The evaluator then determines how much feedback will be returned and returns it starting with the prioritized ordering requested by the predictor. This kind of experimental design matches that of human-in-the-loop feedback in practice where human labeling is costly and figuring out a subset of samples of interest to be annotated is desirable. Another option for feedback types is returning the performance measurements on the increment, which is simply a controlled validation dataset where the actual labels are not released. The amount of feedback tested in the experimental demonstration of KOWL-718 in Section 4.1 includes: 0%, 50%, and 100% feedback ground truth labels of the incremental training set.

## 4.3 Evaluating Tolerance to Nuisance Novelty

The dataset and above measures assess the learning of task-relevant information, and how novel activities are handled over time. It may be of use, as it is in practice, to assess the tolerance of the predictors to certain variables they are desired to be invariant against, such as task-irrelevant information or nuisance novelties. To do this in HAR, the videos may be visually transformed in ways unseen in training and any corresponding change in the above performance measures may be recorded. If they do not encounter a significant change in performance, then they are deemed tolerant to such visual transformations, such as perspective rotation, hue shifts, visual blur, or noise. Otherwise, such transformations that dramatically affect performance can indicate predictor model weaknesses and areas of improvement. This may be assessed such that different novel visual transforms occur over time and thus are part of learning over time. Otherwise, the predictor’s state may be saved and then reloaded in isolation to evaluate how the predictor at that moment would handle the encountered nuisance novelty. The experiment in Section 5.4 takes the latter approach, loading the saved checkpoints of post-feedback internal model state for that increment and then continuing the incremental learning until the next feedback is given using only the visually transformed videos of the original increments’ samples.

## 4.4 A Template for OWL HAR Predictors

Given the above formalization, a template for OWL predictors that manage novelty in a HAR domain may be defined to provide an outline of what such algorithms must include to perform well in practice. Figure 6 shows a template that includes the subtasks of feature representation learn-

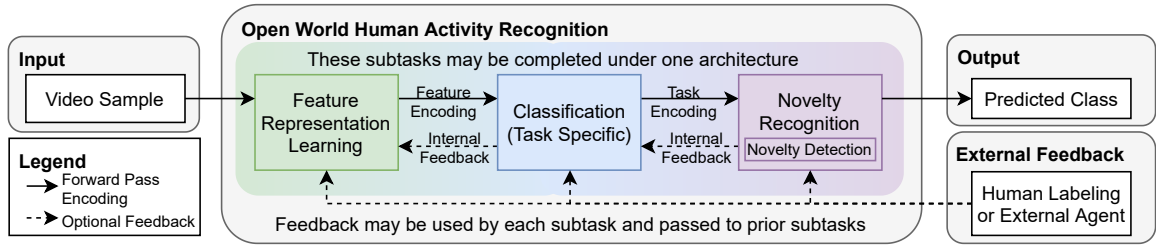


Figure 6: An OWL **predictor template** for HAR with novelty. Learning tasks in an open world requires the subtasks of feature representation, task-specific classification, and novelty recognition to not only detect, but also learn novel classes over time. Feedback is essential to inform the predictor of when to improve at subtasks. Upon request from the predictor, external feedback may be provided from humans as in active learning or from other predictors. See Section 4.4. The models used in our experiments have a frozen feature representation (X3D or TimeSformer) pretrained on Kinetics-400 with a fine-tuned classifier updating every increment when given human labels as feedback. 0%, 50%, and 100% human feedback is examined. More predictor details can be found in Section 5.1.

ing, task-specific classification, and novelty recognition. OWL is inherently a task performed over time. Thus the predictors must account for this and should adapt to novelties that affect task performance (Bendale & Boulton, 2015). These predictors may be able to request external feedback either from human experts as in active learning or from other predictors that are accessible to them.

The first subtask of all OWL predictors for HAR is feature representation learning, which is the learning of the mapping of the input video sample to an informative encoding. As mentioned in Section 2, feature representation plays a key role in not only learning HAR but also detecting and recognizing novel activities.

The second subtask is the classification of known human activities as defined by the task given to this predictor, which means there is a subset of human activities that are task-relevant and use a specific semantic class labeling system. Class labels may differ between datasets and the specific HAR task. The original Kinetics dataset’s evolution from 400 to 700 classes is an example of not only more classes being available over time that are deemed relevant, but also a change in the actual class structure. For example, some samples are labeled as “brushing hair” in Kinetics-400 were given the new label “combing hair” in Kinetics-700 to differentiate between using a brush versus a comb.

The third subtask is handling novelty, which is referred to in Figure 6 as novelty recognition. Novelty recognition includes novelty detection, where being able to detect novelty facilitates the incremental learning of new information, as it is collected over time. In Figure 6, these subtasks are ordered by sequence of typical performance, especially when focused on novel activities. However, novelty recognition can be applied to either the feature encodings from the feature representation space or the task encodings from the task representation space. Performing novelty detection and OWL in the feature representation space is beneficial because it provides more information about the input, however this includes task-irrelevant information and as such nuisance novelties may trigger irrelevant novelty detections and possibly affect novelty recognition performance. When the feature representation learning begins to approach closer to the classification task, task-irrelevant information is naturally lost where task-relevancy is determined by the  $K$  known classes. Perform-



ing novelty detection or recognition within a feature representation space that is closer to the task may result in ignoring novel information, including future task-relevant information.

As noted in Figure 6, these three subtasks may be completed separately by different processing modules or together by one or two modules. The important underlying design is that these subtasks share information with one another and tend to be performed sequentially as ordered here, especially when the novelty of interest is in the class activities.

As part of updating the predictor’s internal state, external feedback may be leveraged, when possible, that is either provided from human annotators as in active learning, or from other predictors. Feedback from human annotators could be labels of the detected unknown classes, labels of notably incorrect samples in the known classes, or some other signal of performance informed by human annotators. Feedback from predictors can be similar or even more nondescript signals of feedback. To properly use this external feedback is a subtask in itself as sometimes the feedback may be in a form that does not directly relate to internal mappings of classes or may even contain noise. As mentioned in Section 4.2, the predictor may request an ordered prioritization of the samples for feedback. The partial feedback of input samples results in semi-supervised updating of the predictor’s internal state.

To enable informed comparison of predictors on a KOWL experiment, we relate the six properties of incremental learning algorithms from (Belouadah et al., 2021) to the terminology we’ve used throughout this paper. If we have a prior introduced term for it, then their term is in parentheses. Otherwise, we use the original names and quote their definitions. We also add a seventh property, “prior knowledge,” as it relates to feature representation learning and is fundamentally an important part to differentiate types of predictors on this benchmark.

1. **Complexity:** “[The] capacity to integrate new information with a minimal change in terms of the model structure.” This refers to the internal state of the predictor, specifically what that state is and how it changes, *e.g.*, the predictor’s number of parameters and changes in their values.
2. **Experience (Memory):** The prior mentioned predictor experience may be limited in memory space. When this is the case, performing OWL for HAR may become more difficult and nuanced as the predictor needs to handle maintaining the key information of the HAR classes and any information of use for differentiating novel from known activities classes.
3. **Regret (Accuracy):** The predictor’s internal assessment of its own performance. This is a separate and possibly similar or entirely different calculation than what the evaluator uses to assess the predictor’s performance.
4. **Timeliness:** “[The] delay needed between the occurrence of new data and their integration in the incremental models.” In the case of the KOWL protocol, the time for the predictor to perform its operations, such as updating its state and performing inference.
5. **Plasticity:** “[The] capacity to deal with new classes that are significantly different from the ones that were learned in the past.” In the case of KOWL experiments, the predictor may require feedback or may be able to learn in a semi-supervised manner.
6. **Scalability:** “[The] aptitude to learn a large number of classes, typically up to tens of thousands, and ensure usability in complex real-world applications.” KOWL-718 has 718 activity classes and the rate of novel classes per increment is rather consistent as seen in Table 1.

7. **Prior Knowledge:** A predictor’s prior knowledge must be *explicitly stated* to know how to properly compare it to other predictors. There are predictors *with no prior knowledge*, *i.e.*, those without any prior training on data external to this benchmark or without Bayesian priors selected through information about how the predictor performed on prior runs of KOWL experiments with the same data. Before the predictor has seen the first sample in the initial step’s training split, the predictor should essentially know nothing, otherwise known as being maximally uncertain (Jaynes, 1968). This is favorable to the scientific method as it preserves the closed system of controlled evaluation of a predictor’s learning on this benchmark data under this protocol.

A predictor *with prior knowledge* may still be evaluated on a KOWL experiment, but we strongly recommend comparing predictors with prior knowledge against those with similar prior knowledge. For example, if there are pre-trainings being used, either use the same pre-training feature representations or be trained on the same external data before starting a KOWL experiment. Otherwise, if the point is still to assess the predictor’s learning of the HAR task within the KOWL experiment, special care needs taken to demonstrate that the prior knowledge is irrelevant to learning the HAR task within the KOWL experiment. If one only cares if their predictor can perform well on the benchmark regardless of informative priors, for example to answer the question of does the prior share information with the benchmark’s task, then of course they are free to do so, but it must be acknowledged that this mode is not assessing the predictor’s learning of the task as represented by the KOWL experiment’s data alone.

All baseline predictors examined in the below experiments have their experience as an unlimited memory buffer in the demonstration examples. This can be treated as an experimental parameter changed when analyzing different predictors on KOWL-718.

## 5. Experimental Demonstration

The following experiments demonstrate the OWL protocol as applied to the Kinetics dataset series to form the KOWL-718 benchmark. Multiple feedback amounts were examined, consisting of 0%, 50%, and 100% feedback as ground truth labels of the incremental training split. The predictors determined the ordering of samples for which to receive feedback. Alongside the standard evaluation as specified in the above protocol, which specifically assesses the incremental open world learning of human activities, we conducted an ablation study of the predictors’ performances given Kinetics-AVA annotations. We also examined the state-of-the-art feature representation tolerance to unseen visual transforms to the Kinetics-400 videos.

### 5.1 HAR Predictors for Evaluation

There were two feature representation models explored in this work: X3D (Feichtenhofer, 2020) and TimeSformer (Bertasius et al., 2021). Both are models with promising performance on the HAR task, and the Kinetics datasets specifically. X3D is a 3D ResNet (He, Zhang, Ren, & Sun, 2016) and TimeSformer is a video transformer (Dosovitskiy, Beyer, Kolesnikov, Weissenborn, Zhai, Unterthiner, Dehghani, Minderer, Heigold, Gelly, Uszkoreit, & Houlsby, 2022). Specific implementation details for these models can be found in Appendix C.2.1. Both models are initialized at their Kinetics-400 pretraining state and the layer just before the softmax readout is used as the feature

representation encoding. Starting with Kinetics-400 pretrainings ensures no information about the future increments is leaked, preserving a controlled incremental learning experiment. We note that X3D and TimeSformer pretrained on Kinetics-400 were trained in a supervised fashion meaning that their feature representation more closely approaches the classification task, containing more task-relevant information as defined by the known classes, but may lack future task-relevant information in the videos yet to be deemed task-relevant at the initial increment.

The fine-tuned classifier that serves as our demonstrative baselines for this OWL HAR benchmark is a single fully connected layer to the feature representation that then outputs to the final softmax classification layer, denoted as “ANN”. The fine-tuned classifier is the only state of the predictor updated during the incremental learning. The ANN classifier always has an unknown class in its softmax classifier and as novel classes become known, the classifier’s output increases in size. Novelty detection is handled using a threshold over the softmax output of the classifier where the initial increment’s validation partition is used to set that threshold with an accepted level of error, which was 10% in these experiments. The accepted level of error represents a prior expectation of how well the validation data is believed to represent the known classes, and was used only to ensure some novelty detection occurred for demonstration purposes. The ANNs have no method of handling novelty recognition, only detection.

Given the ANNs cannot handle novelty recognition, a semi-supervised classifier was used to depict novelty recognition by learning the potential unknown classes. This classifier, denoted “GMM FINCH”, consisted of a Gaussian Mixture Model (GMM) on the feature representation space where the Gaussian components were determined by the FINCH (Sarfraz, Sharma, & Stiefelhagen, 2019) clustering algorithm performed on each class’s sample sets. If the known labels are available, then those samples form different groups of points by class in which FINCH calculated the clusters within each separately. In the hope of better learning the feature representation space’s density for finding unknown classes, a Gaussian distribution was fit over a class’s clusters to form the class’s GMM. Each Gaussian distribution was fit using the uniformly minimum-variance unbiased estimators for its cluster, which is simply the sample mean and covariance in feature representation space. The samples that were deemed unknown served as their own unknown class, which was fit with a GMM in a similar fashion. The unknown samples were based on the predictions of the classifier after being fit after thresholding on the logarithmic probabilities. The threshold was found in a similar fashion to the ANNs using the validation data as all knowns and a hyperparameter to establish an accepted amount of error on knowns in hope of enabling better novelty detection in the future. A sample is deemed novel to the known classes by this threshold if the sample has a logarithmic probability less than the minimum maximum-likely class logarithmic probability minus the likelihood adjustment found from the validation data given the accepted error.

The use of the Extreme Value Machine (EVM) (Rudd, Jain, Scheirer, & Boulton, 2018), which is an open world-specific classifier, was also explored. However, its performance was found to be worse than the ANN on the initial increment and in addition to its memory constraints and runtime issues, it was left out of further incremental learning analysis. The EVM in itself is only a novelty detector and cannot perform novelty recognition on its own. See Appendix C.2.2 for details.

The properties of the predictor baselines used to demonstrate the experimental process using the KOWL-718 benchmark are:

1. **Complexity:** All baseline predictors used fixed feature representations of either X3D or TimeSformer on Kinetics-400. Finetuned ANNs only adjusted their weights when given feed-

back and they involve only one hidden layer. GMM FINCH was updated in a semi-supervised fashion when given unseen data samples, with or without evaluator feedback.

2. **Experience:** All predictors examined have an unlimited memory buffer in the demonstration examples. However, this could be an experimental parameter changed when analyzing different predictors on KOWL-718.
3. **Regret:** The Kinetics-400 pre-trained feature representations used the losses respective to their model, X3D or TimeSformer. Cross-entropy was used to train the finetuned ANNs. GMM FINCH used the logarithmic probability density function for each class’s GMM.
4. **Timeliness:** No time-limits were placed on a predictor’s inference or fitting operations.
5. **Plasticity:** The baseline finetuned ANNs can only detect unknowns. They do not support recognizing unknown classes and must be given feedback labels to account for new activity classes over time. The GMM FINCH predictors learn a GMM in the fixed feature space per activity class and as such may identify unknown classes without feedback as Gaussian distributions within the feature space. The GMM FINCH predictors thus update whenever any new data is presented to it, even without feedback.
6. **Scalability:** All predictors were fit on 407 activity classes in the initial increment and then incrementally encounter the remaining novel 311 classes, totaling 718 classes. The rate of new classes per increment is seen in Table 1. No further assessment of scalability is demonstrated. See Appendix C.2 for implementation details.
7. **Prior Knowledge:** No external prior knowledge was used. Pre-trainings of X3D and TimeSformer on Kinetics-400 were used only to expedite the experimental process by skipping their fitting on the initial increment in KOWL-718, which is the same input data.

Task performance for Kinetics is often measured using classification accuracy of top-1, top-5, or  $1 - \frac{\text{top-1} + \text{top-5}}{2}$ . Given that our unified labeling is inherently imbalanced, we examine not only accuracy, but also Matthews Correlation Coefficient (MCC) and the normalized mutual information (NMI) normalized by the arithmetic mean of entropies as they are measures that better capture performance. They are still affected by class imbalance, but will not have high values for any ill performing cases, such as nearly always predicting the most frequent class.

As mentioned earlier, three feedback amounts were used in the incremental learning of this demonstration, which were 0%, 50%, and 100% feedback using the ground truth labels. 100% human label feedback is the typical supervised incremental learning paradigm where all ground truth labels are given to the predictor after an initial performance assessment at each increment. 0% feedback is when no feedback of any form is given to the predictor and its performance is examined based how well it detects novel classes as unknown, and, if the predictor learns unknown classes over time, how its class mappings correlate to the unknown ground truth. The ANN predictor baselines with 0% feedback do not update under the complete supervised learning paradigm. However the GMM FINCH predictors continue to update in a semi-supervised manner without any further feedback labels. 50% feedback is the most nuanced as the predictor must perform the subtask of requesting feedback for the increment’s sample ordered by some prioritization to better perform the task. Given the small spread of raw performance difference between the 100% and 0% feedback ANNs (see Figure 7), the performance figures depict only GMM FINCH performing 50% feedback for the simplicity of demonstration and the visual readability of the figures.

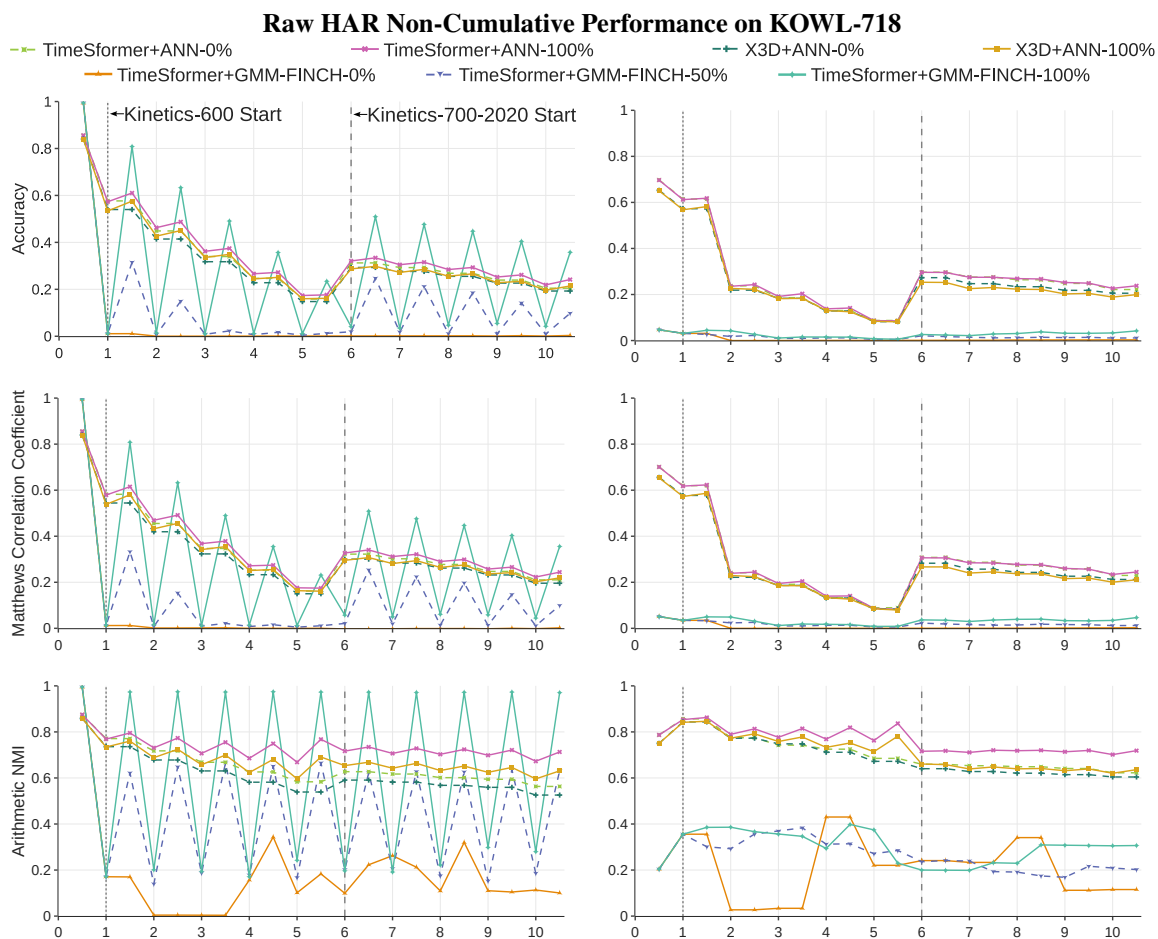


(Fig. 7.1) Training Set

(Fig. 7.2) Testing Set

Figure 7: The **non-cumulative** incremental HAR **raw confusion matrix** performance of the baseline predictors where the incremental evaluation for **pre-feedback is on whole numbers** and **post-feedback is on half steps**. All pre-feedback samples are out-of-sample, regardless of whether they are in the future training data. The raw confusion matrix compares the top-1 predictions to the target label without any reductions of knowns or unknowns. The **predictors were fit on all prior and current experienced data** at each increment, *except* that the ANNs did not use prior seen validation / test sets as unlabeled data as the GMM FINCH recognizer did.

## 5.2 Open World HAR: Novel Activities Over Time

The time-series line plots, such as the figures for the classification task in Figure 8, and the raw unreduced performance in Figure 7, are all non-cumulative point-estimate measurements. This means that every measurement stands for the performance only on the new data for that increment where at the whole step the new data serves to evaluate the generalization of the predictor in the pre-feedback phase and then the half-step evaluates the predictor after being given the feedback requested, if any. Analyzing the performance in a non-cumulative manner indicates the effect that each increment's samples have at that moment in time to better compare the performance on pre- and post- feedback.

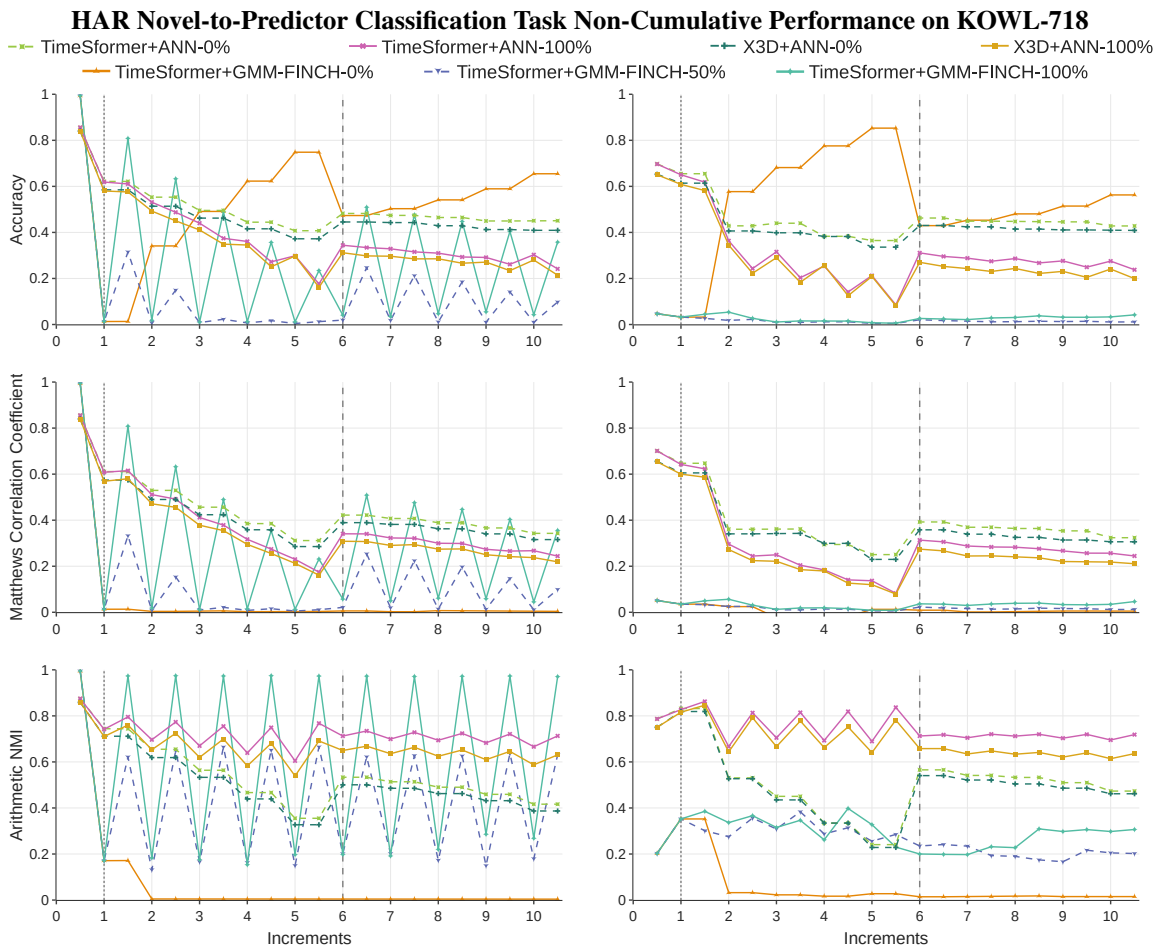


(Fig. 8.1) Training Set

(Fig. 8.2) Testing Set

Figure 8: The **non-cumulative** incremental HAR classification task performance of the baseline predictors where the incremental evaluation for **pre-feedback is on whole numbers** and **post-feedback is on half steps**. All pre-feedback samples are out-of-sample, regardless of whether they are in the future training data. The **predictors were fit on all prior and current experienced data** at each increment, *except* ANNs did not use prior seen validation / test sets as unlabeled data as the GMM FINCH recognizer did. TimeSformer serves as the best feature representation. The ANN with 0% feedback past the initial Kinetics-400 training data performs slightly worse than its incremental learning 100% feedback counterpart. GMM FINCH predictors are found to overfit their data and perform worse than the ANNs. The Kinetics-700 test data is the original dataset’s validation data as no labels for the test data were publicly released. See Section 4 for data specifics. See Figure 7 for the raw confusion matrix plots without any reduction of known or unknown classes.

As such, jumps in performance from one increment to another may occur due to the number of samples and changes in balance of the classes by introducing the increment’s novel classes. The figures for assessing how the predictors handle novelty, such as novelty detection Figure 9, novelty recognition Figure 10, novelty reaction time Figure 11, all only show the performance at the pre-feedback phase, as no novelty occurs in the post-feedback phase given the video samples have already been seen.

### 5.2.1 HAR CLASSIFICATION TASK PERFORMANCE

The HAR primary classification task performance of the incremental learning predictors was assessed over time as novel classes were introduced in each increment, as seen in Figure 8. Note that this includes the reduction of actual unknown and recognized unknown classes into the “unknown” catch-all class. The performance of all predictors degrades over the increments as expected, given that the feature representation is frozen at Kinetics-400 and thus does not contain information about the new classes added within Kinetics-600 and -700. This decrease in performance happens even when 100% feedback is given, indicating that the learned feature representations from X3D and TimeSformer do not generalize to unseen activities given the Kinetics-400 training data to the rest of Kinetics-600 and -700 samples. Otherwise, the classifiers would be able to perform better on the accuracy and MCC measurements in Figure 8. Overall, predictors using the TimeSformer as their feature representation outperformed those using X3D. This increase in performance comes at the cost of longer training and inference times as noted in Appendix C.2.1. Given that TimeSformer consistently outperforms X3D, the plots include only the GMM FINCH predictors using the TimeSformer feature representations for clearer visual readability.

The post-feedback NMI for nearly all of the models using 100% feedback are higher than their relative pre-feedback evaluation measurements with the exception of the NMI of GMM FINCH increment 5. The finetuned ANNs with 0% feedback have the same post-feedback performance as their pre-feedback performance because no updates are made to their internal state after the initial increment. The GMM FINCH with 50% feedback also experiences an increase in performance in the post-feedback phases, but in the training set either not as significant as the 100% feedback and in the testing set not always improving relative to the increment’s pre-feedback measurements. Nonetheless, this supports the belief of the value of informative feedback for learning a task.

Notably, from both Figure 8 and the raw performance in Figure 7, the GMM FINCH model seems to overfit the training data, as indicated by the low measurements during the pre-feedback phases (whole numbers) and high measurements during post-feedback phases (half-steps) on the training set and the low measurements on the both phases in the testing set. The 0% feedback GMM FINCH is an example of when to observe MCC and mutual information because on both the training and testing sets in Figure 8 the accuracy indicates high performance due to predicting unknowns frequently. But doing so does not correlate linearly or non-linearly with the actual labels, as captured by MCC and the normalized mutual information.

The predictors exhibit an interesting phenomena where on post-feedback their accuracy and MCC either remain the same or drop, while the opposite happens for most of their NMI scores. This is due to the fact that at post-feedback the novel classes are no longer reduced to unknown if feedback labels for that class were given to the predictor. The raw measures for these predictors mostly remain similar in performance for post-feedback compared to their pre-feedback, especially the finetuned ANNs, as seen in Figure 7.

Given the reduction of unknowns, the predictors with different feedback amounts have fewer known activities to learn and more samples that fall under “unknown.” Due to this, such predictors may have higher performance measurements as seen in the 0% feedback finetuned ANNs on accuracy and MCC. However the ANN’s NMI indicates they perform worse than their 100% feedback counterparts. Furthermore, referencing the raw confusion matrix’s measures in Figure 7, these increases in accuracy and MCC vanish, indicating it is due to the reduction of unknowns. Also, the GMM FINCH 50% feedback at times exceeds its 100% feedback counterpart on the testing set.

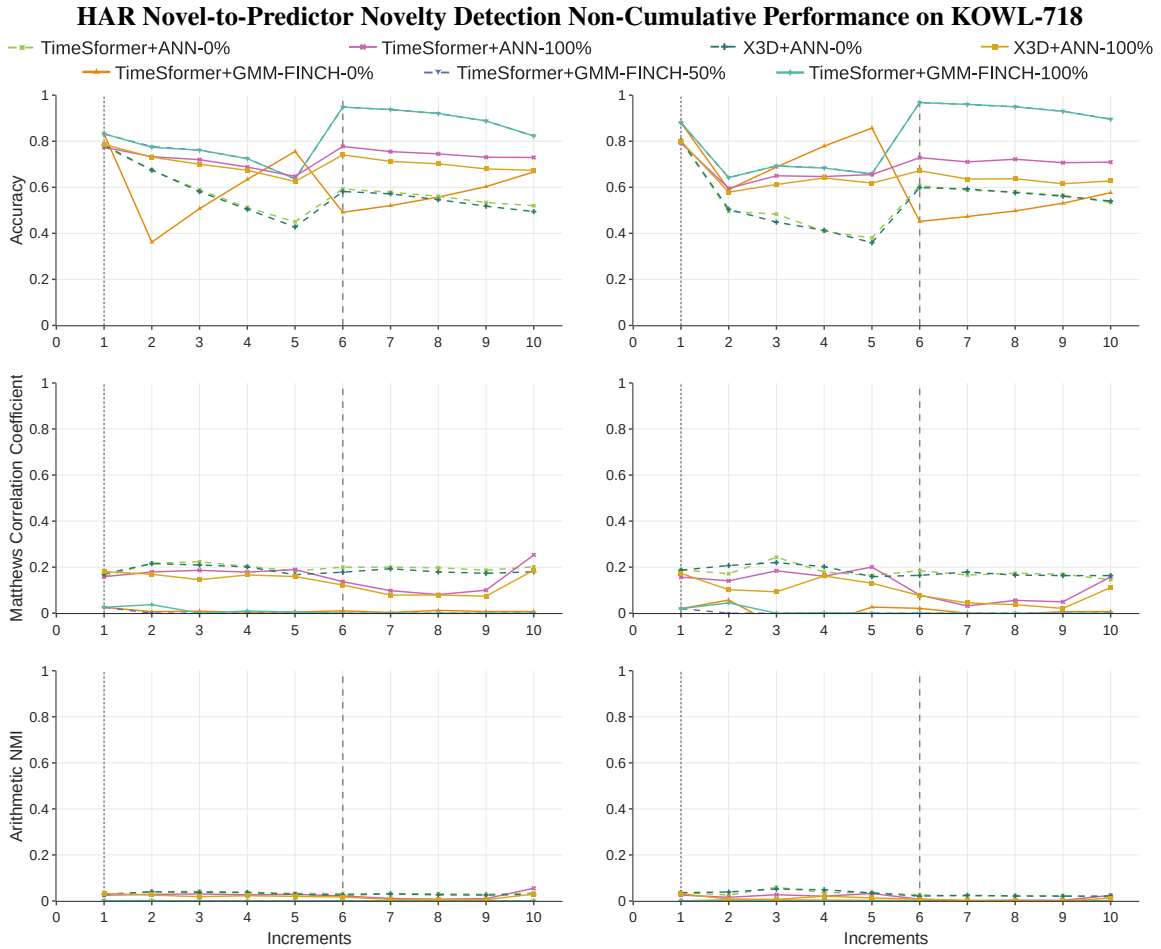


(Fig. 9.1) Training Set

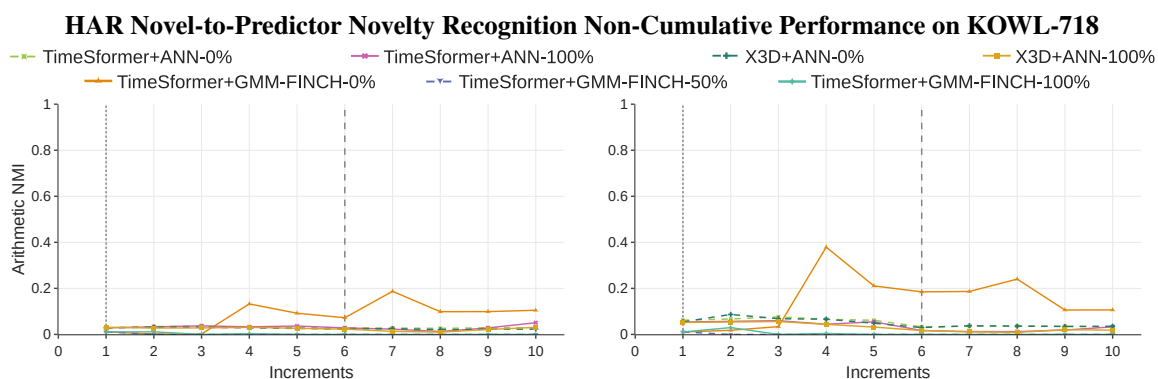
(Fig. 9.2) Testing Set

Figure 9: The novelty detection performance of the predictors over incremental learning on KOWL-718. Both novelty detection and recognition are assessed at the beginning of each increment during the **pre-feedback** phase, and the results are on the combination of **all new data** in that increment’s training or test set. The first observation of an increment’s novel samples is in the pre-feedback phase only. All pre-feedback samples are out-of-sample, regardless of whether they are in the future training data.

### 5.2.2 HAR NOVELTY DETECTION PERFORMANCE

Figure 9 depicts the novelty detection performance of the predictors during incremental learning. This is the binary classification task when the known classes to the predictor at each increment are reduced to “known” and the actual unknowns and predictor’s recognized unknown classes are reduced together to “unknown.” We note that the 100% feedback GMM FINCH’s accuracy is nearly identical to that of the known class frequency shown in Table 1. This means that the GMM FINCH 100% feedback is predicting “known” nearly all the time, which is an ill performing novelty detector and is captured by the low measurements of MCC and NMI. Based on the MCC and NMI measures, the baseline predictors demonstrate that novelty detection over the incremental learning of KOWL-718 is not an easy task, and also demonstrate how accuracy may be misleading. The best novelty





(Fig. 10.1) Training Set

(Fig. 10.2) Testing Set

Figure 10: The novelty recognition non-cumulative performance of the baseline predictors. The first observation of an increment’s novel samples is in the pre-feedback phase only. All pre-feedback samples are out-of-sample, regardless of whether they are in future training data.

detectors in Figure 9 would be the finetuned ANNs using the threshold determined from the initial increment’s validation set. Although demonstrative, the baseline performance leaves much to be desired and indicates room for improvement from future predictors.

### 5.2.3 HAR NOVELTY RECOGNITION PERFORMANCE

Figure 10 depicts the non-cumulative predictor performance as they incrementally learn KOWL-718. Accuracy and MCC are not useful to visualize given that they require the symbolic mappings to be exact mappings, where novelty recognition is inherently a comparison of clustering along with a single catch-all “known” class. At best, accuracy would simply be overly optimistic when predicting samples as known the majority of the time given the balance of knowns to unknowns in KOWL-718, which is representative of real world scenarios. Given this and the amount of samples per increment, the mutual information normalized by the arithmetic mean of entropies is measured per increment to assess the shared task-relevant information between the actual labels and the predictor’s recognized unknown classes. Perhaps as hinted at by the prior novelty detection performance, the baselines do not perform well on novelty recognition with the majority of the NMI measurements for the predictors falling below 0.1. The TimeSformer GMM FINCH with 0% feedback notably outperforms all the others starting from increment 4 onwards, but does not exceed a measurement of 0.4 NMI. This demonstrates the difficulty of the semi-supervised learning task of novelty recognition and we are hopeful that future predictors will surpass these baselines as more researchers take up this line of work.

### 5.2.4 HAR NOVELTY REACTION TIME PERFORMANCE

Figure 11 depicts the novelty reaction time of the predictors on KOWL-718 and indicates that the ANN models with thresholding for unknown samples all react at the same time regardless of their feature representation model. The ANN models react the slowest on the training set as it is released at the pre-feedback stage but join the GMM-FINCH 0% model for the first five increments as the fastest reacting predictors to novelty. The GMM-FINCH with 50% feedback reacts the slowest out of all of the models over all sets, with only the first increment having a notably less than 1.0

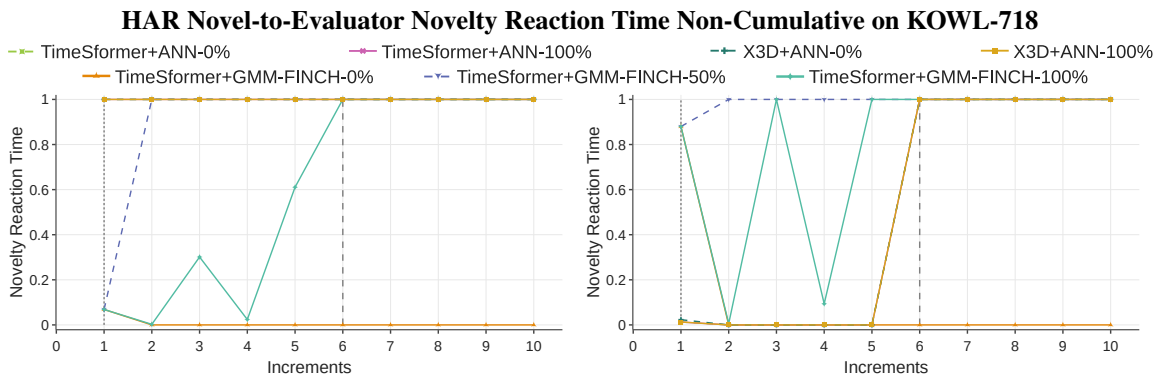


(Fig. 11.1) Training Set

(Fig. 11.2) Testing Set

Figure 11: The per-increment novelty reaction time measure from Equation 1 of the baseline predictors. Unlike the prior measures, the optimum direction here is minimization towards zero. The first observation of an increment’s novel samples is in the pre-feedback phase only. All pre-feedback samples are out-of-sample, regardless of whether they are in future training data. TimeSformer+GMM-FINCH-0% is the best performing on reaction time given its low values, while all of the ANNs perform the worst on the training set. TimeSformer+GMM-FINCH on 50% and 100% feedback has lower reaction times early on in both sets, but joins the ANNs in maximum reaction time value by the 6th increment when the Kinetics-700 dataset begins.

reaction time score. The GMM-FINCH with 100% feedback is the most sporadic in its reaction times as evident in its scores prior to the sixth increment. The GMM-FINCH with 0% feedback consistently has the fastest reaction time of all models. This may be due to tending towards guessing “unknown” in favor of “known,” as the prior MCC and NMI measures in Figure 9 were very low. But its detection accuracy was not too low overall and it did perform the best out of all predictors on novelty recognition, which indicates that out of all of the baseline predictors in this demonstration, it may be a contender for the best model in handling the novelty-related subtasks of HAR.

### 5.3 Ablation Study of Performance given AVA-Kinetics

The measurements so far only examine the performance of the different subtasks given novel human activities occurring in an open world. To better analyze how performance is affected by characteristics of the video samples, an ablation study of the predictors’ classification task performance over KOWL-718 was conducted using annotations from AVA-Kinetics (Li et al., 2020) to examine any difference in performance given certain characteristics of the videos. AVA-Kinetics annotated different types of information for a single key frame on a subset of videos in the Kinetics datasets. Using these annotations, we were able to observe the performance of the predictors under different circumstances, such as the different types of Kinetics actions, the different number of AVA actions occurring within a key frame, the number of humans that were in a key frame of a video, and the amount of pixel area occupied by humans using the arithmetic mean area of their bounding boxes in the key frames. AVA-Kinetics provided a grouping of the Kinetics actions into three types. The AVA actions differ from the Kinetics datasets’ classes, which results in the possibility of multiple classes occurring in a single frame. AVA-Kinetics records the AVA actions as bounding boxes over the humans performing the action. This enables counting the number of AVA actions and humans occurring in a single key frame. The total area of humans within a video was calculated by taking

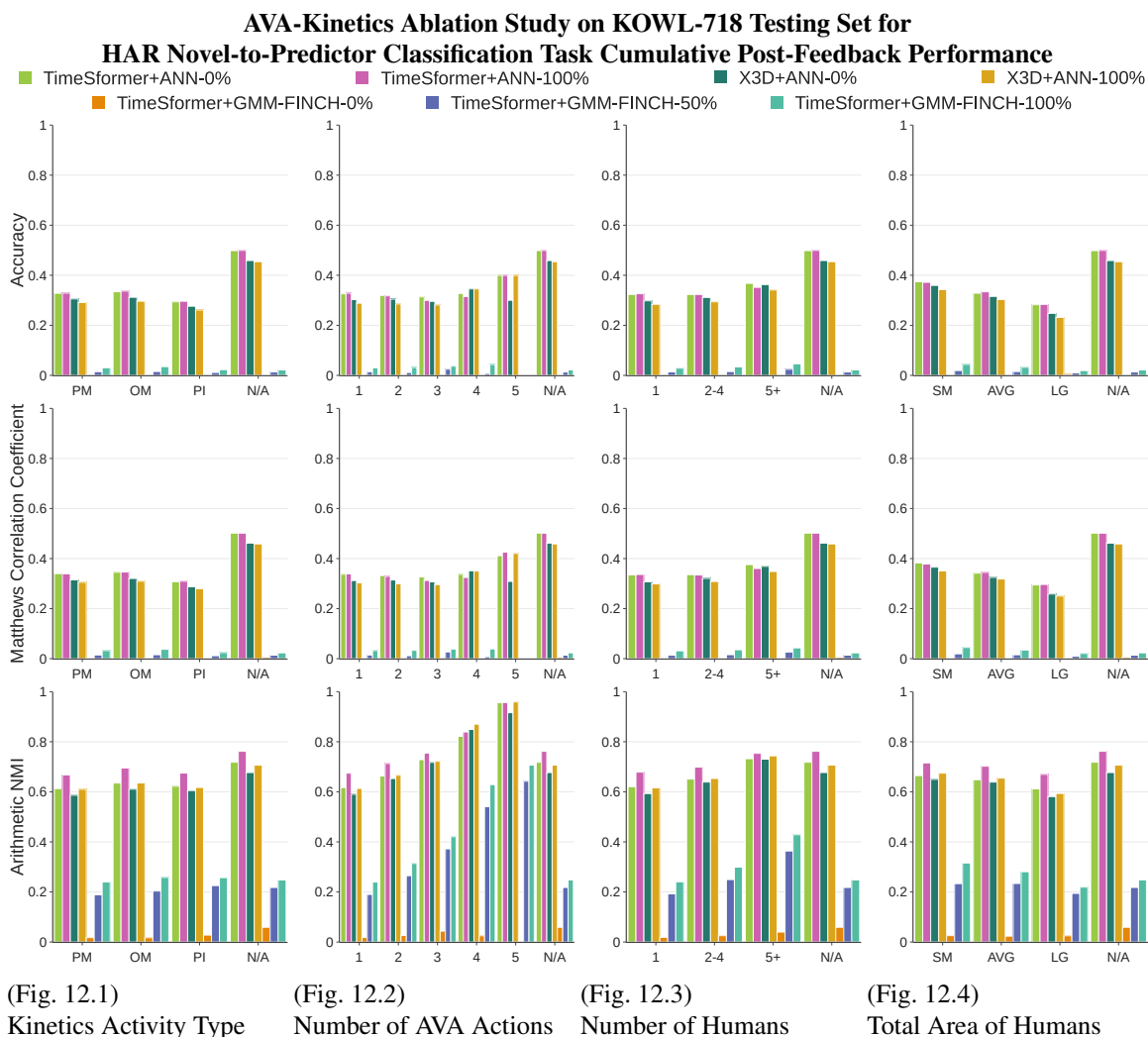


Figure 12: We conducted an ablation study of the classification task **cumulative post-feedback** performance on KOWL-718 under different annotation types using each video’s annotated key frame in AVA-Kinetics (Li et al., 2020). Cumulative means that all of the confusion matrices associated with the time-steps for the post-feedback phase were summed together, adding together the occurrences. AVA-Kinetics only covers a subset of Kinetics videos. Any videos not annotated fall under “N/A”. AVA activity types are: Person Movement (PM), Object Manipulation (OM), and Person Interaction (PI). Total area of humans is the mean of the bounding box areas normalized by the total area of the frame, which was then binned into thirds as small (SM), average (AVG), and large (LG). See Section 5.3 for details and discussion.

the arithmetic mean of the areas associated with the bounding boxes for the key frame. Then those mean areas were binned into “small,” “medium,” and “large,” to enable an easier comparison of the amounts of average area the humans occupied within the frame. To get the bins, the mean areas were put into ascending order split into thirds uniformly over the samples.

Figure 12 depicts the ablation study on cumulative post-feedback performance of the predictors on the HAR novel-to-predictor classification task over KOWL-718. The measures over the three Kinetics Activity Types indicates minimal difference in performance but with Person Interaction

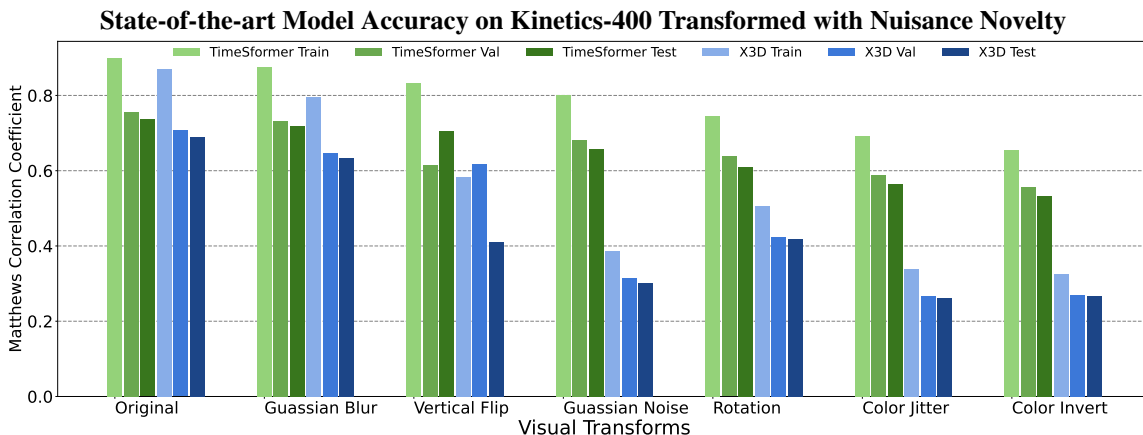


Figure 13: To evaluate tolerance against novel video representations, the HAR accuracy of state-of-the-art models on visually transformed videos was recorded. X3D and TimeSformer pretrained on Kinetics-400 given transformed Kinetics-400 videos both experience a decrease in accuracy when encountering unseen visual transformations. The TimeSformer performed the best in all cases. This shows these models are not invariant to such visual transformations.

activities having slightly worse symbolic performance across all predictors as depicted by accuracy and MCC. The clearest depiction of a difference in performance across the ablation study is the Number of AVA Actions within a single key frame in Fig. 12.2. Especially for Arithmetic NMI, the measured mutual information across all predictors increases as the number of AVA Actions within a key frame increases. There is a subtle increase in the accuracy and MCC of the ANN predictors for five AVA actions versus less than four for AVA actions. This could be due to more AVA actions within a key frame aiding a predictor in classifying the Kinetics activity class, but further detailed analysis and possibly more annotated data would be necessary to support this finding. One possibility is that there are so few samples for the videos with more AVA actions, that they become easier to predict as they are learned. For example, group activities may be more easily determined if the predictors can determine Number of Humans follows a similar, albeit weaker, trend to the Number of AVA Actions, as seen by the measures in Fig. 12.3. Total Area of Humans has a subtle decrease in the performance measures across all predictors as the mean area of the humans in the key frame increases. This could indicate that more visual environmental context may better inform the predictor of the Kinetics activity class. However, it is important to be wary of this as it could also indicate overfitting due to over-dependence on the environment rather than the humans performing the action.

#### 5.4 HAR Predictor Tolerance to Nuisance Novelty

The above evaluation focused on action class specific novelty, however machine learning algorithms are desired to be tolerant to noise, and nuisance novelty is inherently never before seen noise patterns or other phenomena that are task-irrelevant. We assessed the tolerance of pre-existing state-of-the-art models, X3D and TimeSformer, to novel visual representations by examining the performance of these models on Kinetics-400 versus Kinetics-400 with visual transformations not seen during training. The videos are transformed using six different types of visual transformations unseen during training, shown in Figure 14. These transformations were applied to the videos with randomized

## HUMAN ACTIVITY RECOGNITION IN AN OPEN WORLD

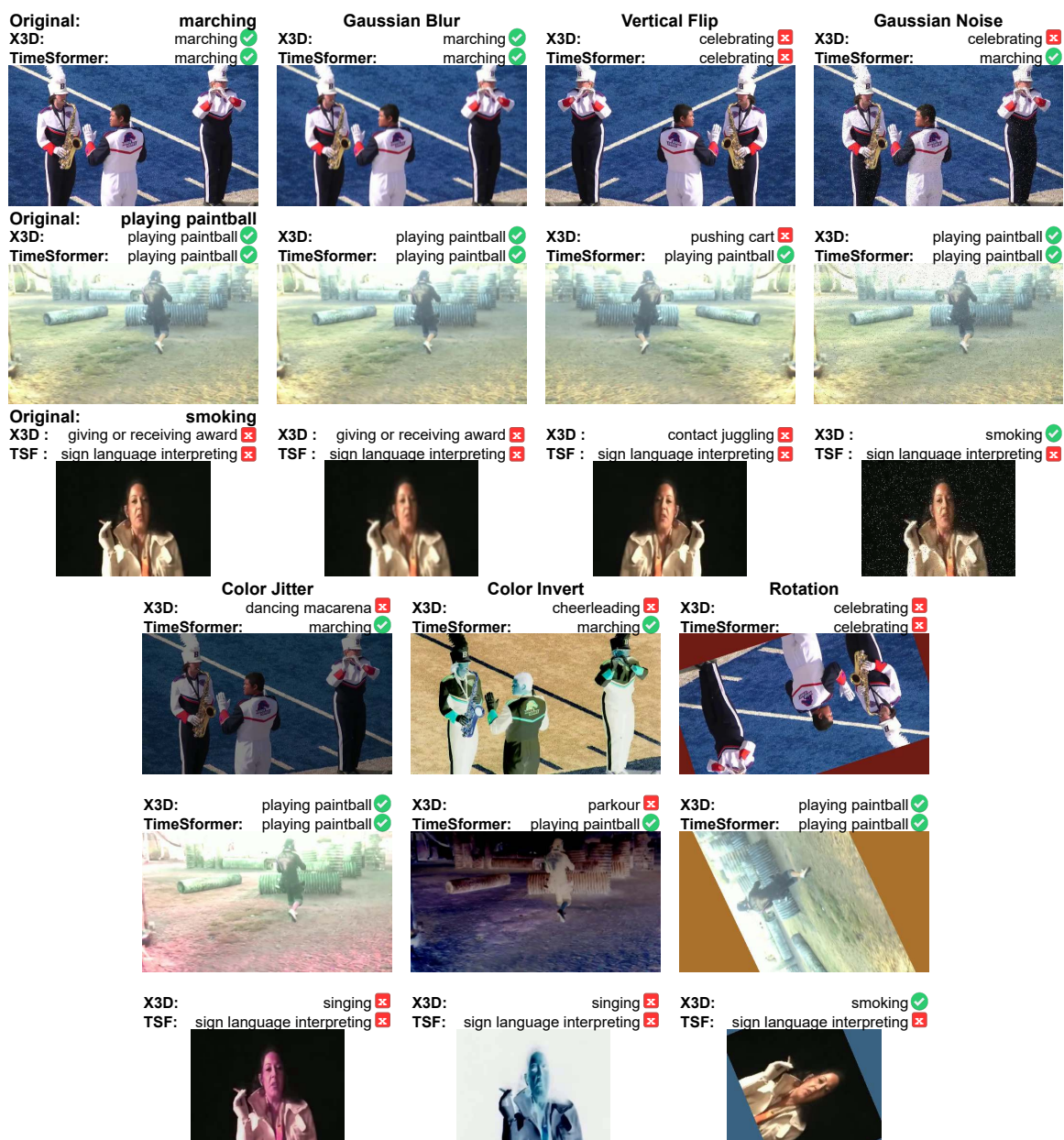


Figure 14: Examples of the visual transforms on Kinetics-400 validation videos unseen by the predictors, along with their X3D and TimeSformer original pre-trained classifier predicted labels marked as correct or incorrect. While not exact matches, the incorrect predictions have an understandable visual misinterpretation in these examples. The actual label was included in the top-5 predictions for all except for the marching example’s X3D on color jitter and TimeSformer on flip and rotation; the playing paintball example’s X3D on flip and color invert; and the smoking example’s X3D on the original, Gaussian blur, and color jitter. TimeSformer always predicted “smoking” as its second most likely guess for the smoking example.

parameters for each transform. The visual transformations were performed such that identical transformations were performed on each frame from the same video, with the exception of noise, which

was random for each frame. The MCC of each predictor for each visual transform is depicted in Figure 13. We find that the Kinetics-400 pretrained X3D and TimeSformer model performance is not invariant to such novel representations, especially color inversion and the rotation of videos. However, TimeSformer performs the best overall and is minimally affected by random Gaussian blur of videos.

## 6. Conclusion

With the increased interest in learning tasks in the face of novelty (Boult et al., 2021; Langley, 2020), we formalized HAR in an open world and provided a reproducible and extendable OWL protocol to evaluate predictors in learning novel classes incrementally over time. Applying this protocol to the popular Kinetics datasets, we constructed a practical benchmark, KOWL-718, that serves as an example of the difficult real world problem of learning human activities from videos as new data becomes available, where unseen actions may be encountered. This benchmark serves to exemplify the nuance in performing HAR in an open world as multiple subtasks are involved and intertwined together. The provided OWL protocol allows for analysis of different aspects of learning HAR in an open world, including varying levels of feedback. Further analysis of predictor performance was recorded when the videos are visually transformed or when the number of people between videos differs. The demonstrative baseline predictors indicate that while the learning of these subtasks together is possible, it is nontrivial to excel at all of the subtasks at the same time. This primes future work on this benchmark which is unlike many others and ripe for further research.

## 7. Acknowledgement

This research was sponsored in part by the National Science Foundation (NSF) grant CAREER-1942151 and by the Defense Advanced Research Projects Agency (DARPA) and the Army Research Office (ARO) under multiple contracts/agreements including HR001120C0055, W911NF-20-2-0005, W911NF-20-2-0004, HQ0034-19-D-0001, W911NF2020009. The views contained in this document are those of the authors and should not be interpreted as representing the official policies, either expressed or implied, of the DARPA or ARO, or the U.S. Government.

## Appendix A. The Three Primary Spaces of Novelty for HAR

The following discussion for HAR follows from the framework introduced in (Boult et al., 2021). The World  $\mathcal{W}$ 's state space is the space of all human activities  $s_{\mathcal{W}} \in \mathcal{S}_{\mathcal{W}}$  and an oracle knows the maximum likely activity class for each activity. A dataset's ground-truth human activity labels along with the paired video serve as samples from the oracle. The samples from the world are used to learn the task and assess performance based on feedback either directly or indirectly from an oracle. The true task in the world is only ever approximated via sampling and it is the job of the oracle and the experimental designers to determine if the predictor is learning that actual task. This means that the world dissimilarity  $\mathcal{D}_{\mathcal{W}}$  and regret measures  $\mathcal{R}_{\mathcal{W}}$  are never truly known, but are approximated via supervised learning when training the predictor. HAR is framed as a discrete classification task where predictors output their predicted nominal class label, and as such the confusion matrix and its derived measures, *e.g.*, accuracy, Matthews Correlation Coefficient (MCC), or Mutual Information or its normalized variants may be used to assess predictor performance at each

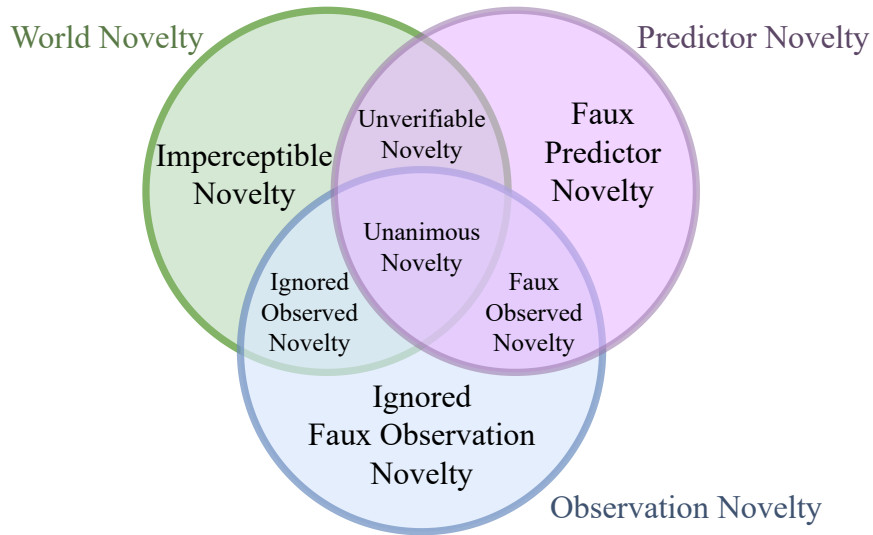


Figure 15: Set representation of novelty spaces adapted from (Boult et al., 2021). We use the term “predictor” in-place of “agent”. See Section 3 and Appendix A.

time-step of learning as the world regret measure  $\mathcal{R}_W$  when inverted. If the order or magnitude of weighting between mutually exclusive activity classes are desired, then the desired output of the predictor is a probability vector assigning probability to each of the known classes and unknown recognized class-clusters. To analyze these, ordered top- $k$  confusion matrices may be used in order to obtain measure such as the top- $k$  accuracy. The world experience  $E_W$  is simply the past sequence of states indexed by the time-step  $t$ . The world state transition function  $\tau_W(t, s_W)$  is the experimental process used to determine the next sample video to give the predictor, based on the current time-step and world state.

The observation space  $\mathcal{O}$  is the encoding of world states after being processed by sensors, resulting in the sensor states  $s_O \in S_O$ . In the case of visual HAR, the sensors are cameras that capture video footage of human activities, so the state space consists of the video frame with its color space. The observation dissimilarity measure  $\mathcal{D}_O$  tends to be Euclidean distance or the difference of video pixel values between frames. However, this dissimilarity function is very literal and captures any and all changes in pixels or frames. If the observation space is instead designed to ignore more task-irrelevant changes, then a different dissimilarity measure may be used. For example, in the case of smart cameras that may represent the sensor input in some encoding learned by an artificial neural network, the dissimilarity measure used can be the inverse of cosine similarity. The standard for most annotated HAR datasets is to not assess the quality or noise introduced by the video camera beyond possibly noting that noise exists or classes are imbalanced. Fully simulated environments lend themselves best to this kind of assessment given that it requires multiple human annotations to assess real world samples for video quality, noise, and the presence of other novelties.

The observation regret measure  $\mathcal{R}_O$  is the regret the predictor could have given the available information in this space. This differs from the world regret measure because it does not necessarily include all of the information that the world space contains. This regret measure is only applied in practice when the experimental designers consider and address the difference in information between the world space and the observation space.  $\mathcal{R}_O$  is not directly applied in this paper’s

experiments as it is determined by the sensors used to capture the videos and would be expressed by meta-data or further annotations of the videos. The observation experience  $E_{\mathcal{O}}$  is the time-step indexed history of prior sensor states, which is the videos in HAR. In the case of real world applications, the  $E_{\mathcal{O}}$  may have a limited capacity to store the prior states, and so this may be defined as a buffer and thus forgotten states will be deemed novel if encountered again. The oracle or experimental designer may know the truth in such a case, and assess the predictor with this knowledge. The observation state transition function  $\tau_{\mathcal{O}}(t, s_{\mathcal{W}})$  is the transformation of the given world state through the sensors that form the observation space.

The predictor space  $\hat{\mathcal{Y}}$  is the space of the predictor’s model and states  $s_{\hat{\mathcal{Y}}} \in \mathcal{S}_{\hat{\mathcal{Y}}}$ . The HAR predictor makes decisions or predictions about the activity labels, but depending on setup of experiments and available data, may request feedback. The predictor’s dissimilarity measure  $\mathcal{D}_{\hat{\mathcal{Y}}}$  may be cosine similarity, Euclidean distance, or any measure that applies to the predictor’s encoded space of the activity phenomena. The predictor’s regret measure  $\mathcal{R}_{\hat{\mathcal{Y}}}$  tends to be its objective function, *e.g.*, loss function, regret function, or a heuristic. The predictor’s experience  $E_{\hat{\mathcal{Y}}}$  is often limited by physical and practical constraints given it is a computer program, thus it may be in practice a finite sized memory buffer. In this paper’s experiments using Kinetics, we did not encounter physical limits of the memory buffer. The predictor’s state transition function  $\tau_{\hat{\mathcal{Y}}}(t, s_{\mathcal{O}}, s_{\hat{\mathcal{Y}}})$  takes the given observation state and performs HAR predicting the human activity class while also detecting novelty and optionally updating its state.

## Appendix B. Formalism: HAR Novelty Set Relations

With defined novelty spaces for HAR, we may further specify the types of novelty encountered in this domain following (Boult et al., 2021). Given the three novelty spaces, the presence of novelty across them forms set relationships as visualized in Figure 15. The entire list of defined sets of novelty given the three novelty spaces for HAR is as follows:

**Unanimous Novelty:** This is novelty that occurs in the world, is observable via the sensors, and is detected by the predictor. This is the True Positive case of novelty detection. For example, correctly detecting the first “blowdrying hair” sample or “swimming with dolphins” sample in Figure 1.

**Imperceptible Novelty:** Novelty that occurs in the world but is unable to be sensed by the sensors. In HAR, this can be wavelengths of light that are unable to be sensed, such as infrared or ultra violet light that cannot be recorded with an RGB sensor. This could also include novelty that is not within the camera’s field of view or is occluded, which could affect the activity being recorded. For example, in a multi-person team sport, if something happens off camera that causes all teammates to stop and stare, then the cause of them staring is a novelty imperceptible to the camera.

**Ignored Observed Novelty:** Observed novelty that is ignored by the predictor because it is deemed as task-irrelevant or because the predictor is simply unable to interpret the novelty in its input. The ironing hair example from Figure 1 is a case where the predictor sees hair being brushed, but does not recognize the hair iron given it is not task-relevant based on the prior known classes and data.

**Ignored Faux Observation Novelty:** This is novelty that is introduced in the observation novelty space that is ignored by the predictor and thus not deemed as a novelty to it. An example is



when the predictor is tolerant to hue shifts in the visual input that occur due to sensor error and performs as expected on the HAR task.

**Faux Observed Novelty:** In contract to Ignored Faux Observation Novelty, Faux Observed Novelty is novelty that originates in the observation novelty space but is also detected as novelty by the predictor and thus is included in the predictor novelty space. Following the hue shift from the prior example, this is when the predictor is not tolerant to hue shifts and detects them as novelty.

**Faux Agent Novelty:** This is when the predictor falsely detects novelty in its input space (feature space), otherwise known as a False Positive novelty detection. In Figure 1, if the third video of “walking the dog” was classified as a novel human activity class, this would be the agent misunderstanding the visual input of three dogs on a leash as a new class. Perhaps seeing three dogs together is novel, but in this case the human activity is still known and the presence of more dogs results in a nuisance novelty.

**Unverifiable Novelty:** This is when a predictor correctly detects novelty in the state, but this cannot be confirmed by the predictor because the sensors cannot sense this novelty. This occurs when the predictor makes a lucky guess, leverages latent knowledge about that task, or uses knowledge external to what was found in the sensors, such as prior knowledge included by human designers. If a camera’s point of view misses a novelty that has occurred off camera, then at that moment of time it cannot verify that novelty occurred or exists, but may be able to do so later in the future by simply shifting its point of view.

## Appendix C. Additional Experiment Details

### C.1 Data Specifics

Collecting the Kinetics Dataset is unfortunately not straight forward for such a standard benchmark. The data is officially distributed by Google as a list of YouTube IDs. This means that a large portion of it has fallen victim to link rot where the links are broken and the videos are no longer available, especially in the older Kinetics 400 and 600 sets. Fortunately, there are at least two other sources for this data, a torrent for Kinetics-700<sup>2</sup> and Kinetics-400<sup>3</sup>, and a repository hosted by the CVDF<sup>4</sup>. These two sources offer a significantly more complete version of the dataset, and are convenient ways to download the files. This paper used the repository hosted by the CVDF. Information about the specific samples that were missing in our experiments is available in the project’s source repository and supplemental data files.

See Table 2 for the breakdown of total number of samples used and activity classes per increment, as well as their original source Kinetics dataset that was used to construct KOWL-718.

### C.2 Predictor Specifics

#### C.2.1 FEATURE REPRESENTATION MODEL DETAILS

**X3D Details** The X3D (Feichtenhofer, 2020) model used in this work uses a pure pytorch implementation of X3D Multigrid (Wu, Girshick, He, Feichtenhofer, & Krahenbuhl, 2020), found at: <https://github.com/kkahatapitiya/X3D-Multigrid>. We used the pretrained weights for the “M” model trained on Kinetics 400 in the official distribution from FAIR found

2. <https://academictorrents.com/details/49f203189fb69ae96fb40a6d0e129949e1dfec98>

3. <https://academictorrents.com/details/184d11318372f70018cf9a72ef867e2fb9ce1d26>

4. <https://github.com/cvdfoundation/kinetics-dataset>

Source Dataset	K-400	Kinetics-600					Kinetics-700-2020				
Increments	0	1	2	3	4	5	6	7	8	9	10
<b>Train</b>											
Known											
classes	409	409	455	501	547	593	636	653	670	687	704
samples	218371	16082	19148	24661	32391	44687	34287	36112	38527	41855	47128
Novel											
classes	0	46	46	46	46	43	17	17	17	17	14
samples	0	3163	5513	7730	12298	25538	1870	2415	3331	5273	10144
<b>Validate</b>											
Known											
classes	409	409	455	501	547	593	636	653	670	687	704
samples	18016	333	20	45	88	156	4892	4990	5197	5473	5883
Novel											
classes	1	46	46	46	46	43	17	17	17	17	14
samples	0	75	72	68	75	124	163	208	277	411	684
<b>Test</b>											
Known											
classes	409	409	455	501	547	593	0	0	0	0	0
samples	35256	795	287	446	644	940	0	0	0	0	0
Novel											
classes	1	46	46	46	46	43	0	0	0	0	0
samples	1	104	160	198	297	488	0	0	0	0	0

Table 2: The resulting number of known and novel classes and their samples **per increment** for the Kinetics-400, -600, and -700-2020 datasets using the configuration in Section 5: most recent label first, first come first assigned data split, and most frequent novel class first per future dataset. The Kinetics datasets unfortunately experienced link rot and some original samples have been lost. The single novel class and its single sample in Kinetics-400 test is still included in KOWL-718, but Table 1 excluded it for brevity.

in (Fan, Li, Xiong, Lo, & Feichtenhofer, 2020). The reported performance of this model is as follows: Top-1 10 view: 75.1, Top-1 30 view: 76.1. The aforementioned repo’s model zoo from which we pulled the weights can be found at [https://github.com/facebookresearch/SlowFast/blob/main/MODEL\\_ZOO.md](https://github.com/facebookresearch/SlowFast/blob/main/MODEL_ZOO.md) ported into Kahatapitiya’s pure PyTorch implementation. After porting the weights, we were able to approximately verify the model’s performance on our version of Kinetics 400, with some variance due to issues such as dataset collection difficulties and differences in video preprocessing, our performance is shown in MCC as “Original” in Table 3

**TimeSformer Details** The TimeSformer feature extractor used in this work was adapted from the Kinetics-400 reference model distributed by (Bertasius et al., 2021) from <https://github.com/facebookresearch/TimeSformer>. Specifically, we used the one labeled as “TimeSformer” for which they gave the following statistics: number of frames: 8, spatial crop: 224, top 1 accuracy: 77.9, top 5 accuracy: 93.2. The code was only modified to return the feature embedding from the encoder as an additional output. The raw TimeSformer result in MCC are shown in the “Original” row of Table 3

### C.2.2 FINETUNED CLASSIFIER MODEL DETAILS

The primary finetuned classifier models include an ANN that takes as its input the feature representation of the samples and outputs a softmax classifier output, which is the unknown class with the currently known classes together as a probability vector. The ANNs used for both of the feature representation models was a fully connected dense network of one hidden layer with a LeakyReLU activation that then went to the softmax classifier layer which was sized as known classes + 1 for the unknown catch-all class. In experimentation to find a suitable ANN architecture, multiple hidden layers and hidden layer widths were examined, including multiple layers with skip connections through concatenation. In the end, the single hidden layer model with the same size as the feature representation vector was found to be the most performant, using a dropout during training of 0.5 probability. We also explored different numbers of total training epochs ranging from [1, 100]. We found that 100 epochs would result in overfitting, as seen in Fig. 16, which compares the performance of the Finetuned ANN for 100 epochs versus the original logit predictions of the feature representation’s original classifier layer output. The runtimes of the 100 epochs ANN was approximately 8 hours of wall time on the Kinetics-400 dataset only using Kinetics-400 labels. The runtime of the single epoch ANN was approximately 1 half-hour of wall time for the incremental learning experiment at the cost of an estimated 0.05 MCC performance loss based on the training run on only the Kinetics-400 data.

An Extreme Value Machine (EVM) was also evaluated. However, as seen in Fig. 16, the EVM performed worse than the ANN on the HAR task. Given this in addition to its longer computation time, we excluded it from the experiment in the main paper. Given that Kinetics-400 does is not necessarily representative of Kinetics-600 and -700, ee note that the EVM may have resulted in better novelty detection performance over the incremental learning than the base finetuned ANN without any further novelty handling than a single unknown class included at each time-step. The EVM’s runtime on the Kinetics-400 only training totaled approximately 16 hours with a loss of performance relative to both the feature representations’ original classifiers and the fine-tuned ANN.

Given time constraints and resource limitations, we only trained the finetuned classifier ANN in the incremental learning with 1 epoch per increment. The ANN trained with 1 epoch on Kinetics-400 was found to be somewhat less performant than when trained with 100 epochs. The perfor-

F. Repr.	Classifier	Train	Val.	Test
X3D	Original	0.8701	0.7067	0.6893
X3D	ANN 100	<b>0.9891</b>	0.7054	0.6890
X3D	ANN 1	0.8414	0.6929	0.6740
X3D	ANN 1 + EVM	0.5777	0.4836	0.4698
TSF	Original	0.8988	<b>0.7548</b>	<b>0.7361</b>
TSF	ANN 100	<i>0.9817</i>	<i>0.7546</i>	<i>0.7344</i>
TSF	ANN 1	0.8566	0.7410	0.7237
TSF	EVM	0.5552	0.4995	0.4938

Table 3: The HAR **classification task** performance as measured by MCC on **Kinetics-400 with its original labels** comparing different feature representation and classifier combinations of the predictor. The Original uses the X3D’s (Feichtenhofer, 2020) and TimeSformer’s (Bertasius et al., 2021) (TSF) original classifier layers with pretrained weights. These MCC values correspond to the bar chart in Fig. 16.

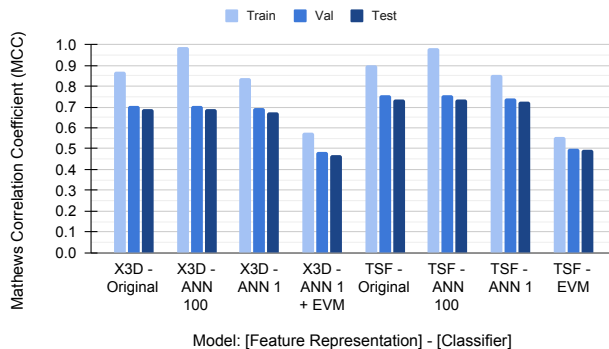


Figure 16: The Extreme Value Machine (EVM) (Rudd et al., 2018) was less performant with a longer run-time to fit of about 8 hr. The ANN 100 was a fully connected ANN with a single hidden layer trained for 100 epochs, which cost about the same time as the EVM to fit. The ANN fit with only 1 epoch took dramatically less run-time to fit and predict versus the rest at the cost of less than a  $\sim 2\%$  decrease in validation and test performance to the original classifier layer.

mance was still acceptable as a baseline for the primary HAR task as seen in the main text for incremental learning performance.

### C.2.3 HARDWARE, RESOURCES, AND COMPUTATIONAL RUNTIMES

These models were run on a variety of compute resources. In order to facilitate experimentation, we first ran feature extraction on the entire unified datasets (KOWL-718) with both the X3D and TimeSformer models. A full run of the feature extraction takes approximately 30 hours for the X3D feature extractor and approximately 23 days for the TimeSformer feature extractor when using an Nvidia Quadro RTX 6000. In order to speed up the wall clock time of this process, we broke the dataset into 60 equal sized batches which each took about 30 minutes and 9 hours on the RTX 6000 respectively and ran the batches in parallel.

## C.3 Predictor Tolerance to Nuisance Novelty

In order to evaluate how the models held up to spurious representation novelty, we evaluated model performance after the video was modified using a number of common visual transformation techniques. This meant that we needed to run a full pass on the unified dataset, KOWL-718, for each of the 6 types of visual transformations. This resulted in approximately 194 GPU days for feature extraction.

Once feature extraction was completed, the computational cost for the Kinetics 400 visual transform assessment became quite low in Section 4.3. During the feature extraction process, the extracted features were saved to reduce the overhead of running experiments multiple times. Without saving the state, the compute overhead would have been substantially higher.

## References

- Beddiar, D. R., Nini, B., Sabokrou, M., & Hadid, A. (2020). Vision-based human activity recognition: a survey. *Multimed Tools Appl*, 79(41), 30509–30555.
- Belouadah, E., Popescu, A., & Kanellos, I. (2021). A comprehensive study of class incremental learning algorithms for visual tasks. *Neural Networks*, 135, 38–54.
- Bendale, A., & Boulton, T. (2015). Towards Open World Recognition. In *Conference on Computer Vision and Pattern Recognition*, pp. 1893–1902.
- Bertasius, G., Wang, H., & Torresani, L. (2021). Is Space-Time Attention All You Need for Video Understanding?. In *Proceedings of the 38th International Conference on Machine Learning*, pp. 813–824. PMLR. ISSN: 2640-3498.
- Boulton, T. E., Cruz, S., Dhamija, A. R., Gunther, M., Henrydoss, J., & Scheirer, W. J. (2019). Learning and the Unknown: Surveying Steps toward Open World Recognition. *Proceedings of the AAAI Conference on Artificial Intelligence*, 33(01), 9801–9807. Number: 01.
- Boulton, T., Grabowicz, P., Prijatelj, D., Stern, R., Holder, L., Alspector, J., Jafarzadeh, M. M., Ahmad, T., Dhamija, A., Li, C., Cruz, S., Shrivastava, A., Vondrick, C., & Walter, S. (2021). Towards a Unifying Framework for Formal Theories of Novelty. *Proceedings of the AAAI Conference on Artificial Intelligence*, 35(17), 15047–15052. Number: 17.
- Brighi, M., Franco, A., & Maio, D. (2021). ActivityExplorer: A semi-supervised approach to discover unknown activity classes in HAR systems. *Pattern Recognition Letters*, 151, 340–347.
- Carreira, J., Noland, E., Banki-Horvath, A., Hillier, C., & Zisserman, A. (2018). A Short Note about Kinetics-600. *arXiv:1808.01340 [cs]*, ””. arXiv: 1808.01340.
- Carreira, J., Noland, E., Hillier, C., & Zisserman, A. (2019). A Short Note on the Kinetics-700 Human Action Dataset. *arXiv:1907.06987 [cs]*, ””. arXiv: 1907.06987.
- Chalmers, D. J. (2006). Strong and weak emergence. In *The Re-Emergence of Emergence: The Emergentist Hypothesis from Science to Religion*, pp. 244–415. OUP Oxford. Google-Books-ID: gQZREAAAQBAJ.
- Cover, T. M., & Thomas, J. A. (1991). *Elements of Information Theory*. Wiley Series in Telecommunications. John Wiley & Sons, Inc., New York, USA.
- Dhamija, A. R., Ahmad, T., Schwan, J., Jafarzadeh, M., Li, C., & Boulton, T. E. (2021). Self-Supervised Features Improve Open-World Learning. *arXiv:2102.07848 [cs]*, ””. arXiv: 2102.07848.
- Dosovitskiy, A., Beyer, L., Kolesnikov, A., Weissenborn, D., Zhai, X., Unterthiner, T., Dehghani, M., Minderer, M., Heigold, G., Gelly, S., Uszkoreit, J., & Houlsby, N. (2022). An Image is Worth 16x16 Words: Transformers for Image Recognition at Scale. In *International Conference on Learning Representations*.
- Fan, H., Li, Y., Xiong, B., Lo, W.-Y., & Feichtenhofer, C. (2020). Pyslowfast. <https://github.com/facebookresearch/slowfast>.
- Feichtenhofer, C. (2020). X3D: Expanding Architectures for Efficient Video Recognition. In *Proceedings of the IEEE/CVF Conference on Computer Vision and Pattern Recognition*, pp. 203–213.

- Geng, C., Huang, S.-J., & Chen, S. (2021). Recent Advances in Open Set Recognition: A Survey. *IEEE Transactions on Pattern Analysis and Machine Intelligence*, 43(10), 3614–3631. Conference Name: IEEE Transactions on Pattern Analysis and Machine Intelligence.
- Gershman, S. J., & Niv, Y. (2015). Novelty and Inductive Generalization in Human Reinforcement Learning. *Topics in Cognitive Science*, 7(3), 391–415. eprint: <https://onlinelibrary.wiley.com/doi/pdf/10.1111/tops.12138>.
- Gutoski, M., Lazzaretti, A. E., & Lopes, H. S. (2021). Deep metric learning for open-set human action recognition in videos. *Neural Comput & Applic*, 33(4), 1207–1220.
- He, K., Zhang, X., Ren, S., & Sun, J. (2016). Deep Residual Learning for Image Recognition. In *Proceedings of the IEEE Conference on Computer Vision and Pattern Recognition*, pp. 770–778.
- Ho, C.-H., & Vasconcelos, N. (2020). Contrastive Learning with Adversarial Examples. *arXiv:2010.12050 [cs]*, "" . arXiv: 2010.12050.
- Inácio, A. D. S., Gutoski, M., Lazzaretti, A. E., & Lopes, H. S. (2021). OSVidCap: a Framework for the Simultaneous Recognition and Description of Concurrent Actions in Videos in an Open-Set Scenario. *IEEE Access*, "", 1–1. Conference Name: IEEE Access.
- Jaynes, E. T. (1968). Prior Probabilities. *IEEE Transactions on Systems Science and Cybernetics*, 4(3), 227–241. Conference Name: IEEE Transactions on Systems Science and Cybernetics.
- Kay, W., Carreira, J., Simonyan, K., Zhang, B., Hillier, C., Vijayanarasimhan, S., Viola, F., Green, T., Back, T., Natsev, P., Suleyman, M., & Zisserman, A. (2017). The Kinetics Human Action Video Dataset. *arXiv:1705.06950 [cs]*, "" . arXiv: 1705.06950.
- Kinney, J. B., & Atwal, G. S. (2014). Equitability, mutual information, and the maximal information coefficient. *PNAS*, 111(9), 3354–3359.
- Langley, P. (2020). Open-World Learning for Radically Autonomous Agents. *AAAI*, 34(09), 13539–13543.
- Li, A., Thotakuri, M., Ross, D. A., Carreira, J., Vostrikov, A., & Zisserman, A. (2020). The AVA-Kinetics Localized Human Actions Video Dataset. *arXiv:2005.00214 [cs, eess]*, "" . arXiv: 2005.00214.
- Losing, V., Hammer, B., & Wersing, H. (2018). Incremental on-line learning: A review and comparison of state of the art algorithms. *Neurocomputing*, 275, 1261–1274.
- Masana, M., Liu, X., Twardowski, B., Menta, M., Bagdanov, A. D., & van de Weijer, J. (2021). Class-incremental learning: survey and performance evaluation on image classification.. *arXiv:2010.15277 [cs]*.
- Minh Dang, L., Min, K., Wang, H., Jalil Piran, M., Hee Lee, C., & Moon, H. (2020). Sensor-based and vision-based human activity recognition: A comprehensive survey. *Pattern Recognition*, 108, 107561.
- Pang, G., Shen, C., Cao, L., & Hengel, A. V. D. (2021). Deep Learning for Anomaly Detection: A Review. *ACM Comput. Surv.*, 54(2), 38:1–38:38.
- Qiu, X., Sun, T., Xu, Y., Shao, Y., Dai, N., & Huang, X. (2020). Pre-trained models for natural language processing: A survey. *Sci. China Technol. Sci.*, 63(10), 1872–1897.

- Radford, A., Kim, J. W., Hallacy, C., Ramesh, A., Goh, G., Agarwal, S., Sastry, G., Askell, A., Mishkin, P., Clark, J., Krueger, G., & Sutskever, I. (2021). Learning Transferable Visual Models From Natural Language Supervision. *arXiv:2103.00020 [cs]*, "" . arXiv: 2103.00020.
- Rebuffi, S.-A., Kolesnikov, A., Sperl, G., & Lampert, C. H. (2017). iCaRL: Incremental Classifier and Representation Learning. In *Proceedings of the IEEE Conference on Computer Vision and Pattern Recognition (CVPR)*, pp. 2001–2010.
- Roitberg, A., Al-Halah, Z., & Stiefelhagen, R. (2018). Informed Democracy: Voting-based Novelty Detection for Action Recognition. *arXiv:1810.12819 [cs]*, "" . arXiv: 1810.12819.
- Roitberg, A., Ma, C., Haurilet, M., & Stiefelhagen, R. (2020). Open Set Driver Activity Recognition. In *2020 IEEE Intelligent Vehicles Symposium (IV)*, pp. 1048–1053. ISSN: 2642-7214.
- Rudd, E. M., Jain, L. P., Scheirer, W. J., & Boulton, T. E. (2018). The Extreme Value Machine. *IEEE Transactions on Pattern Analysis and Machine Intelligence*, 40(3), 762–768.
- Ruff, L., Kauffmann, J. R., Vandermeulen, R. A., Montavon, G., Samek, W., Kloft, M., Dietterich, T. G., & Müller, K.-R. (2021). A Unifying Review of Deep and Shallow Anomaly Detection. *Proceedings of the IEEE*, 109(5), 756–795. Conference Name: Proceedings of the IEEE.
- Sarfraz, S., Sharma, V., & Stiefelhagen, R. (2019). Efficient Parameter-Free Clustering Using First Neighbor Relations. In *Proceedings of the IEEE Conference on Computer Vision and Pattern Recognition (CVPR)*, pp. 8934–8943.
- Scheirer, W. J., Rocha, A. d. R., Sapkota, A., & Boulton, T. E. (2013). Toward Open Set Recognition. *IEEE Transactions on Pattern Analysis and Machine Intelligence*, 35(7), 1757–1772.
- Schiappa, M. C., Rawat, Y. S., & Shah, M. (2022). Self-Supervised Learning for Videos: A Survey. *arXiv:2207.00419 [cs]*, "" .
- Smaira, L., Carreira, J., Noland, E., Clancy, E., Wu, A., & Zisserman, A. (2020). A Short Note on the Kinetics-700-2020 Human Action Dataset. *arXiv:2010.10864 [cs]*, "" . arXiv: 2010.10864.
- Tishby, N., Pereira, F. C., & Bialek, W. (1999). The Information Bottleneck Method. *The 37th annual Allerton Conference on Communication, Control, and Computing*, "", 368–377. arXiv: physics/0004057.
- Wu, C.-Y., Girshick, R., He, K., Feichtenhofer, C., & Krahenbuhl, P. (2020). A Multigrid Method for Efficiently Training Video Models. In *Proceedings of the IEEE Conference on Computer Vision and Pattern Recognition (CVPR)*, pp. 153–162.
- Zaeemzadeh, A., Bisagno, N., Sambugaro, Z., Conci, N., Rahnavard, N., & Shah, M. (2021). Out-of-Distribution Detection Using Union of 1-Dimensional Subspaces. In *Proceedings of the IEEE/CVF Conference on Computer Vision and Pattern Recognition*, pp. 9452–9461.